IN THE UNITED STATES PATENT AND TRADEMARK OFFICE

In re the Application of: **TSAO, Betty P. et al.** **Serial No.:** 09/909,317 **Filed:** July 18, 2001 **For: GENETIC MARKER TEST FOR LUPUS**	**Examiner:** Johannsen, Diana B. **Group Art Unit:** 1634 **Docket No.:** 42778.8013.US01 I hereby certify that this correspondence (along with any referred to as being attached or enclosed) is being deposited this 18th day of August 2005 with the United States Postal Service as first class mail in an envelope addressed to the Mail Stop AF, Commissioner for Patents, P.O. Box 1450, Alexandria, VA 22313-1450. Rena Iov

DECLARATION UNDER 37 C.F.R. 1.132 BY JEROME I. ROTTER

Mail Stop AF
Commissioner for Patents
P.O. Box 1450
Alexandria, VA 22313-1450

1. I, Jerome I. Rotter, M.D. of 8700 Beverly Boulevard, # 665 West, Los Angeles, California 90048, am a co-inventor of U.S. Patent Application Serial No. 09/909,317, which is a continuation-in-part of U.S. Application Serial No. 09/280,181, filed on March 29, 1999. I am currently the Director of Research at the Medical Genetics Institute of Cedars-Sinai Medical Center. I hereby declare as follows:

2. I am aware that In an Amendment and Response for the present application dated May 17, 2005, generic terminology and descriptive information was added to the specification and claims to describe the trademarked dyes YO-PRO-1 and SYBR GREEN I.

3. I am aware that In the Amendment and Response of May 17, 2005, the phrase "quinolinium,4-[(3-methyl-2(3H)-benzoxazolylidene) methyl]-1-[3-(trimethylammonio) propyl]-, diiodide (Molecular Probes, Inc.)" was added to the specification to describe YO-PRO-1, and the phrase "quinolinium,4-[(3-methyl-2(3H)-benzoxazolylidene) methyl]-1-[3-(trimethylammonio) propyl]-, diiodide" was added to the claims to describe YO-PRO-1.

4. I am aware that In the Amendment and Response of May 17, 2005, the phrase "a cyclic-substituted unsymmetrical cyanine dye that emits at 519nm when excited at 494nm, Chemical Abstract Service Registry Number CAS 163795-75-3, *Chemical Abstracts, 13th Collective Chemical Substance Index* [1992-1996]) (Molecular Probes, Inc., Eugene, OR)" was added to the specification to describe SYBR GREEN I, and the phrase "a cyclic-substituted unsymmetrical cyanine dye with Chemical Abstract Service Registry Number CAS 163795-75-3" was added to the claims to describe SYBR GREEN I.

5. I am aware that an Amendment and Response is being submitted in conjunction with the present Declaration. This Amendment and Response amends the description of SYBR GREEN I in the specification to read "a dye with an excitation maximum of 494nm and an emission maximum of 521nm, Chemical Abstract Service Registry Number CAS 163795-75-3, *Chemical Abstracts, 13th Collective Chemical Substance Index* [1992-1996]) (Molecular Probes, Inc., Eugene, OR)." This Amendment and Response also amends the description of SYBR GREEN I in the claims to read "the dye with Chemical Abstract Service Registry Number CAS 163795-75-3."

6. I hereby declare that the chemical name "quinolinium,4-[(3-methyl-2(3H)-benzoxazolylidene) methyl]-1-[3-(trimethylammonio) propyl]-, diiodide" corresponded to the trademarked term YO-PRO-1 at the earliest priority date of the present application. This is supported by the reference Sbih-Lammali, F., et al. 1999. Cancer Research 59:924-930, a copy of which is submitted herewith. The supporting language, which is located at pages 925-926, is highlighted in the submitted copy.

7. I hereby declare that the description of SYBR GREEN I as "a dye with an excitation maximum of 494nm and an emission maximum of 521nm, Chemical Abstract Service Registry Number CAS 163795-75-3, *Chemical Abstracts, 13th Collective Chemical Substance Index* [1992-1996]) (Molecular Probes, Inc., Eugene, OR)" was applicable to the trademarked term SYBR GREEN I at the earliest priority date of the present application. A copy of the Chemical Abstracts 13th Collective Chemical Substance Index (1992-1996) entry for SYBR GREEN I is submitted herewith. This reference establishes that the CAS number for SYBR GREEN I prior to the earliest priority date of the present application was 163795-75-3. One of the references cited in the Chemical Abstracts entry, Skeidsvoll, J. and Ueland, P.M. 1995. Anal Biochem 231:359-365, establishes that SYBR GREEN I was known to have an excitation maximum of 494 nm and an emission maximum of 521 nm prior to the earliest priority date of the present invention. A copy of this reference, with the relevant supporting language at page 361 highlighted, is submitted herewith.

8. I hereby declare that all statements made herein of my own knowledge are true and all statements made based on references are believed to be true. All statements herein are made with the knowledge that willful false statements and the

like are punishable by fine, imprisonment, or both under Section 1001 of Title 18 of the United States Code, and that such willful false statements may jeopardize the validity of United States Application No. 09/909,317 and/or any patents issued thereon.

Executed and signed on July 31, 2005, at Los Angeles, California.

Jerome I. Rotter, M.D.

[CANCER RESEARCH 59, 924–930, February 15, 1999]

Control of Apoptosis in Epstein Barr Virus-positive Nasopharyngeal Carcinoma Cells: Opposite Effects of CD95 and CD40 Stimulation[1]

Fatima Sbih-Lammali, Bernard Clausse, Hector Ardila-Osorio, Roland Guerry, Monique Talbot, Séverine Havouis, Laurent Ferradini, Jacques Bosq, Thomas Tursz, and Pierre Busson[2]

Laboratoire de Biologie des Tumeurs Humaines, UMR 1598 Centre National de la Recherche Scientifique [F. S-L., B. C., H. A-O., R. G., S. H., L. F., T. T., P. B.], and Laboratoire d'Histopathologie A [M. T., J. B.], Institut Gustave Roussy, 94805 Villejuif, France.

ABSTRACT

The expression and function of CD95 and CD40 were investigated in malignant cells from EBV-positive undifferentiated nasopharyngeal carcinomas (NPCs). Large amounts of CD95 and CD40 expression were detected in 15 of 16 EBV-positive NPC specimens. In contrast, CD95 was not detected in two biopsies from patients with EBV-negative differentiated NPCs. We tested whether the CD95 apoptotic pathway was functional in NPC cells by treating two EBV-positive NPC tumor lines *in vitro* with a CD95 agonist. In both cases, NPC cells were extremely susceptible to CD95-mediated apoptosis, despite strong constitutive expression of Bcl-x. Combined CD40 and CD95 stimulation was used to investigate the possible anti-apoptotic activity mediated by CD40. The CD40 receptor was activated by incubating NPC cells with murine L cells producing CD154, the CD40 ligand. This treatment resulted in a strong inhibition of CD95-related cytotoxicity. Such an anti-apoptotic effect of CD40 is well known for B lymphocytes, but has not previously been reported for epithelial cells. These data suggest that NPC tumor-infiltrating lymphocytes, which often produce the CD40 ligand *in situ*, may increase the survival of malignant cells, thereby enhancing tumor growth in patients.

INTRODUCTION

Undifferentiated NPCs[3] are rare in most countries; however, their incidence is high in South China and North Africa. Regardless of patient origin, NPCs are consistently are associated with EBV, whose genome is contained in malignant epithelial cells. Several EBV proteins, including EBNA1, LMP1, and the BARF0 protein, are consistently expressed in NPC and probably contribute to the malignant phenotype (1, 2). Small deletions of chromosome 3p and the loss of $p16^{LNK4}$ expression by homozygous gene deletion or, more often, by abnormal gene methylation are the most frequent genetic changes reported in NPC (3, 4). In contrast to most epithelial malignancies, there is a very low frequency of p53 mutations in NPC (5). NPC primary tumors are infiltrated heavily by nonmalignant lymphocytes. Approximately 60% of NPC tumor-infiltrating leukocytes are mature $CD3^+$ T lymphocytes, 15% are CD20-positive B lymphocytes, and ~10% are cells of monocyte/macrophage lineage (6). We previously reported a series of NPC cell characteristics that are potentially important for lympho-epithelial interactions: the constitutive production of IL-1α and constitutive expression of CD40, CD54, and HLA class II molecules (7–9).

There are several lines of evidence supporting the idea that malignant cells are more prone to apoptosis in NPCs than in other head and neck carcinomas. NPCs often are more susceptible than squamous cell carcinomas to radiotherapy and chemotherapy, especially at early stages of the treatment (10, 11). In addition, despite their short doubling time *in situ*, NPC cells adapt poorly to culture *in vitro* or even to transplantation into nude or SCID mice (8, 12). This suggests that critical survival factors from the tumor microenvironment protect NPC cells from apoptosis. We therefore investigated in NPC cells the expression and function of CD95 and CD40, which are key determinants of apoptosis and cell survival in various cell types.

CD95 (also called Fas or Apo1) is an M_r 43,000 transmembrane cell surface receptor of the tumor necrosis factor receptor family. The binding to CD95 of anti-CD95 antibodies or its cognate ligand, CD95L, rapidly induces apoptosis in sensitive cells both *in vitro* and *in vivo* (13). Cell death results from a signaling cascade involving molecules such as the FADD protein and a series of cysteine proteases, particularly caspases 8 and 3 (14). The functional importance of the CD95 system was first recognized in immune systems. It plays a key role in the control of the immune response, particularly in the deletion of autoreactive clones, and is involved in the killing of antigenic target cells by cytotoxic T cells and in the maintenance of immune privilege in organs such as the eye and the testis (15, 16). Constitutive expression of CD95 and CD95L has been observed in a variety of mouse and human tissues with high rates of apoptotic cell death, suggesting that the CD95 system may also be involved in apoptotic cell death during physiological cell turnover (17, 18). Such a mechanism has been demonstrated in female reproductive organs in mice (19). Finally, there are abundant data showing that the CD95 pathway is activated and induces apoptosis in response to a wide range of cellular aggressions in both malignant and nonmalignant cells. This pathway probably is involved in the lethal response to hypoxia (20). Some anticancer drugs, such as doxorubicin, induce production of the CD95 ligand in their target cells. This molecule may then interact with CD95, resulting in autocrine cell suicide (14). In summary, the expression of the CD95 receptor coupled with a functional apoptotic signaling pathway probably significantly increases cell susceptibility to various challenges, including attack by CTLs, hypoxia, radiotherapy, and chemotherapy.

CD40 is an M_r 48,000 membrane receptor of the tumor necrosis factor receptor family. It is activated by CD154, its membrane-bound cognate ligand. CD40 was described initially as a B-lymphocyte activation antigen, but is now known to be expressed by a variety of other cell types, especially endothelial and epithelial cells (21, 22). In human B lymphocytes and dendritic cells, CD40 activation antagonizes CD95-mediated apoptosis (23, 24). We and others have reported previously that malignant NPC cells have consistent and intense membrane expression of CD40, but no precise function has been assigned to this receptor and its ligand in NPCs (8, 25, 26).

We report here that malignant NPC cells strongly express the CD95 receptor and that both CD95 and CD40 are functional in short-term *in vitro* assays in EBV-positive NPC tumor lines. The stimulation of CD95 induces rapid apoptosis. However, prior stimulation of CD40 results in a dramatic reduction of NPC cell apoptosis following CD95 activation. This is the first report of CD40-ligand activation protecting malignant cells of epithelial origin against CD95-mediated apoptosis.

Received 8/7/98; accepted 12/18/98.

The costs of publication of this article were defrayed in part by the payment of page charges. This article must therefore be hereby marked *advertisement* in accordance with 18 U.S.C. Section 1734 solely to indicate this fact.

[1] This work was supported by the Association pour la Recherche contre le Cancer (Grant 9112) and the Comité des Yvelines de la Ligue Nationale contre le Cancer (Grant 034–97).

[2] To whom requests for reprints should be addressed, at Laboratoire de Biologie des Tumeurs Humaines, Institut Gustave Roussy, 94805 Villejuif Cedex, France. Phone: 33-1-42-11-45-83; Fax: 33-1-42-11-54-94; E-mail: pbusson@igr.fr.

[3] The abbreviations used are: NPC, nasopharyngeal carcinoma; FDA, fluorescein diacetate.

MATERIALS AND METHODS

NPC Tumor Lines. Four EBV-positive undifferentiated NPC tumor lines, C15, C17, C18, and C19, were propagated by s.c. passage in nude mice (8, 9). C15 was established from the primary nasopharyngeal tumor of a 13-year-old girl. The other tumor lines were derived from cutaneous (C17) and cervical lymph node (C18 and C19) metastases. C17 and C18 were established from recurrent lesions after irradiation and several courses of chemotherapy.

NPC Biopsies. Frozen biopsies from 14 NPCs collected at the Institut Gustave Roussy (Villejuif, France) were included in this study. Patients were mainly from Algeria, Italy, and France (Table 1). The WHO type was determined in each case by examination of H&E-stained sections. EBV DNA was detected by Southern blotting of tumor DNA for eight specimens (using the *Bam*HI W fragment of the EBV genome as a probe; data not shown). No EBV DNA was detected in biopsies 9 and 10, which were well-differentiated NPCs (WHO type I and II) from French patients. It was not possible to perform a Southern blot for biopsies 4–7. However these patients had typical EBV serological markers and undifferentiated type III NPC. Therefore, these biopsies were classified as EBV-positive.

Antibodies. CD95 and CD40 were detected by flow cytometry or staining of tissue sections with the purified monoclonal antibodies UB2 and MAB 89, respectively (both IgG1; Immunotech, Marseille, France). Tumor-infiltrating leukocytes were stained with an anti-CD45 (Leukocyte Common Antigen, Dako-LC; Dako, Trappes, France). 7C11 (IgM; Immunotech) was used as a CD95 agonist with strong apoptosis-inducing activity. Surface HLA class I molecules were stained with the ATCC W6–32 antibody. An anti-Bcl-x polyclonal antibody (S-18) from Santa Cruz Biotechnology (Santa Cruz, CA) and an anti-Bcl-2 monoclonal antibody from Dako (clone 124) were used for Western blotting.

Immunohistology. Specimens were sectioned at 5 μm and placed on SuperFrost/plus slides (Menzel-Glaser, Braunschweig, Germany) without any fixative. Cryostat sections were incubated with anti-CD95 (UB2), anti-CD40 (MAB 89), or anti-CD45 (Dako-LC) at 2, 2, and 4 μg/ml, respectively, for 1 h at 37°C. Immunoreactivity was detected using a biotin-conjugated antimouse goat antibody followed by an avidin-peroxidase complex (Biostain kit; Biomeda, Foster City, CA). Peroxidase was revealed with the chromogen AEC (3-amino-9-ethyl carbazole), and sections were counterstained with Harris's hematoxylin.

NPC Cell Dispersion and Flow Cytometry Analysis. C15 and C17 were cut into 1 mm^3 fragments and incubated with 8 mg/g tumor collagenase (Worthington, Freehold, NJ) and 20 μg/g tumor DNase I (Sigma, Saint Quentin Fallavier, France), in RPMI containing 20% FCS at 37°C for 3 h. Collagenase-digested fragments were homogenized, and the resulting cell suspension was filtered through a nylon cell strainer with 70 μm pores to remove cell aggregates. Cells were stained indirectly with the appropriate primary antibodies and FITC-conjugated goat antimouse $F(ab')_2$ (Jackson ImmunoResearch, West Grove, PA) and then analyzed using a FACScalibur flow cytometer (Becton Dickinson, Franklin Lakes, NJ).

Table 1 *CD95 and CD40 staining on tissue sections*

Biopsy[a]	Origin	WHO type	EBV DNA	CD95[b]	CD40[b]
1	Algeria	III	+	+	+
2	Algeria	III	+	+	+
3	Algeria	III	+	++	+
4	Italy	III	ND[c]	++	+
5	France	III	ND	+	ND
6	Bulgaria	III	ND	+	ND
7	Italy	III	ND	+	+
8	Algeria	III	+	+	+
9	Algeria	II	−	−	+
10	France	I	−	+/−	+
11	Italy	III	+	++	+
12	Algeria	III	+	++	+
13	Algeria	III	+	++	+
14	France	II	+	+	+/−
		Nude Mouse Tumor Lines			
C15	Morocco	III	+	+	+
C17	France	III	+	++	+
C18	Algeria	III	+	−	−
C19	Italy	III	+	++	+

[a] Patients 4–7 had typical EBV serological markers.
[b] ++, strong plasma membrane staining of all malignant cells; +, moderate staining of the majority of malignant cells; +/−, faint staining of a minority of malignant cells.
[c] ND, not determined.

Short-Term Culture of NPC Cells. NPC cells derived from tumor xenografts were seeded at 5×10^5 cells/well in positively charged 24-well plates (Primaria; Becton Dickinson). They were incubated in RPMI containing 10% FCS, at 37°C in a 5% CO_2 atmosphere. When these experimental conditions were used, >90% of the NPC cells were attached on the plastic support after 1–2 h incubation, with ~60% confluence. Most cells were round. There was no significant cell proliferation; the percentage of cells in $S+G_2$ phases dropped from 15 to 7% in 12 h (data not shown). During the first 24 h, NPC cell loss was <10% and fibroblast contamination remained minimal. However NPC cell survival decreased significantly beyond 24 h, and it was not possible to make additional passages *in vitro*, in part because of major contamination by mouse fibroblasts. All of the experimental procedures reported here were performed within 18 h after tumor cell dispersion.

Anti-CD95 Antibody-mediated Apoptosis. The cells were incubated for 2 h in culture conditions, and the purified 7C11 antibody was added to the treated cell wells. Purified nonspecific mouse IgM was used as a negative control. Cells were incubated with antibodies for 10–14 h, and were then collected by aspiration of the culture medium and trypsin treatment. Viable cells were counted by trypan blue exclusion. CD95-specific cytotoxicity was calculated as the percentage decrease in viable cells in treated wells *versus* nontreated wells. NPC cells were also collected for apoptotic DNA fragment and oligonucleosome assays.

Detection of Apoptotic DNA Fragments and Oligonucleosomes. We detected apoptotic DNA fragments by extracting DNA using the salting out procedure (27). Briefly, 2×10^6 cells were incubated overnight at 37°C in a lysis buffer containing 10 mM Tris-HCl (pH 8.0), 2 mM EDTA, 400 mM NaCl, 0.6% SDS, and 166 μg/ml proteinase K. After digestion, the salt concentration was raised to 1 M for NaCl and 10 mM for $MgCl_2$ and the tubes were shaken vigorously. Samples were centrifuged at 7000 g for 20 min at room temperature, the supernatants were collected, 2.5 volumes of ethanol were added, and DNA was precipitated overnight at −20°C. The DNA was resuspended in Tris-EDTA buffer, treated by DNase-free RNase, and subjected to electrophoresis in a 2% agarose gel. Oligonucleosomes were detected by a sandwich ELISA with antihistone and anti-DNA monoclonal antibodies according to the manufacturer's recommendations (Cell Death Detection ELISA plus; Boehringer, Meylan, France).

Assessment of Viable NPC Cells under CD40 and CD95 Stimulation. CD40 stimulation of NPC cells was achieved by cocultivation with murine L-cells transfected stably with the CD40 ligand gene (kindly provided by Dr. Francine Brière, Schering-Plough, Dardilly, France; Ref. 28). The presence of the CD40 ligand at the cell surface was checked by flow cytometry (data not shown). The tumor was dispersed, and NPC cells were mixed with CD40L-transfected or control untransfected L cells in 24-well plates (2.5×10^5 L-cells and 5×10^5 NPC cells per well). Cocultivated cells were incubated for 6–8 h prior to CD95 stimulation, and then treated with the 7C11 antibody for 10–14 h. At the end of the incubation, the following procedure, based on flow cytometry analysis, was used to count viable human NPC cells. All cells were harvested by aspiration of the culture medium and trypsin treatment. The resulting cell suspension was incubated with the anti-HLA I antibody W6–32 and Cy5-labeled goat antimouse IgG as a secondary antibody (Jackson Immunochemicals). W6–32 did not react with the murine H2 antigen; therefore, only cells of human origin were labeled with Cy5. Viable cells were labeled specifically by activation of FDA before flow cytometry (5 min incubation with 2 mg/ml FDA). Cells labeled with both Cy5 and activated FDA were counted using a FACScalibur flow cytometer (Becton Dickinson). A red diode emitting at 535 nm and a laser argon beam emitting at 480 nm were used to excite Cy5 and fluorescein, respectively. A minimum of 100,000 events was collected for each sample. The sample volumes used for cytometry were determined so that an absolute count of viable NPC cells could be obtained for each sample.

Assessment of Apoptotic NPC Cells under CD40 and CD95 Stimulation. The above-described procedure used for counting viable cells was modified to count cells undergoing apoptosis. Two changes were introduced: (a) cells were collected earlier after the beginning of CD95 stimulation (~8 h later); and (b) in the final step, instead of FDA, cells were stained with 5 μM YO-PRO-1 iodide (quinolinium, 4-{(3-methyl-2(3H)-benzoxazolylidene)-

methyl)}-1{(3(trimethyl-ammonio) propyl}-, diiodide; Molecular Probes, Eugene, OR). YO-PRO-1 is a nucleic acid stain that emits green fluorescence, which passes through the plasma membranes of apoptotic cells even when they are still viable, *i.e.*, when they have undergone changes in membrane permeability but no major membrane breaks (29, 30). Excitation by the red diode (535 nm) and the laser argon beam (480 nm) was used for Cy5 and YO-PRO-1 iodide, respectively. Cells with reduced forward scatter or strong side scatter (dead cells) and negative W6–32 staining (murine cells) were gated out. The remaining YO-PRO-1-positive cells were assumed to be apoptotic, but still viable, NPC cells.

Western Blot Analysis of Bcl-2 and Bcl-x Expression. NPC tumor pieces were disrupted in lysis buffer [150 mM NaCl, 50 mM Tris (pH 7.4), 5 mM EDTA, 0.1% SDS, 0.5% sodium deoxycholate, 0.5% NP40, 0.5 mM Pefabloc] at 4°C, using a conical pestle glass grinder. The lysate was further homogenized by sonication with a microtip probe and clarified by centrifugation for 15 min at 10,000 × *g*. A sample of this protein extract (40 μg) was electrophoresed in a 10% polyacrylamide gel. Western blotting was performed on PVDF membranes (Immobilon P; Millipore, Saint Quentin en Yvelines, France) according to standard protocols. The enhanced chemiluminescence system was used to visualize bound peroxidase-conjugated secondary antibodies, according to the manufacturer's recommendations (Amersham, Les Ulis, France).

RESULTS

CD95 and CD40 Surface Expression on Transplanted NPC Cells. CD95 surface expression was demonstrated in NPC tumor lines by flow cytometry after tumor cell dispersion (C15 and C17) and by immunohistochemistry (C15, C17, C18, and C19). CD95 labeling was very intense on C15 and, to a lesser extent, on C17 cells (Fig. 1). The labeling of C15 and C17 cells was consistently brighter than that of Jurkat (T-cell leukemia) and A431 (squamous cell carcinoma) cell lines. Malignant cells of the C19 tumor were labeled for CD95 by immunohistochemistry. In contrast, the C18 tumor was unstained for CD95 (Table 1). Similar results were obtained for CD40. It was detected in C15, C17, and C19 cells, but not in C18 cells (Table 1 and Fig. 1).

CD95 and CD40 Expression in NPC Biopsies. CD95 expression was analyzed on tissue sections from 14 biopsies. Twelve of these biopsies were derived from typical EBV-associated undifferentiated or poorly differentiated NPCs (WHO type III or II; EBV detected in tumor tissue and/or typical EBV serological markers). All these biopsies tested positive for CD95 (Table 1 and Fig. 2). In contrast, CD95 staining was negative or very weak for two EBV-negative, more differentiated NPCs (WHO type I or II; Table 1, *biopsies 9* and *10*). In the biopsies testing positive for CD95, most of the malignant epithelial cells were stained. In contrast, there was no significant staining of tumor-infiltrating lymphocytes. The expression of CD40 was investigated in 12 biopsies from the same series; malignant cells were labeled strongly in all but one case (*biopsy 14*), including the two EBV-negative carcinomas (Table 1). Some tumor-infiltrating lymphocytes were also positive. These results are consistent with those of previous studies (8, 25, 26).

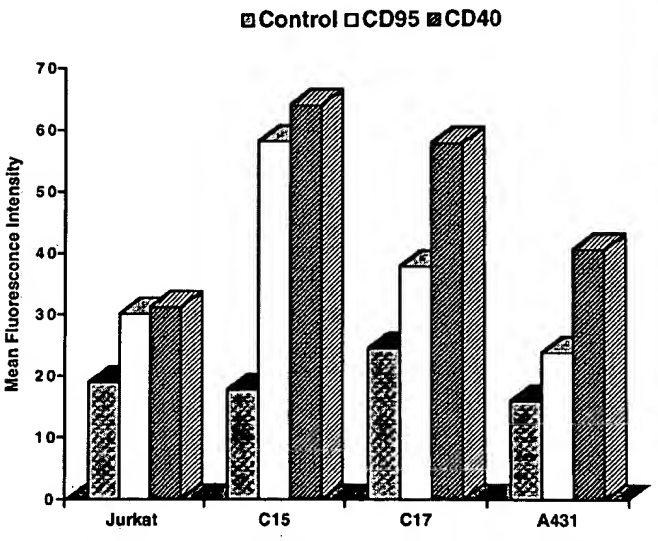

Fig. 1. Flow cytometry analysis of CD95 and CD40 expression on cells derived from the C15 and C17 NPC tumor lines. Negative control samples were incubated with purified mouse IgG1 (10 μg/ml; Sigma, France). CD95 and CD40 molecules were stained with the UB2 (10 μg/ml) and the MAB 89 (5 μg/ml) antibodies. Fluorescence intensities were determined after subtraction of the dead cells stained with propidium iodide. Similar results were obtained in three independent experiments.

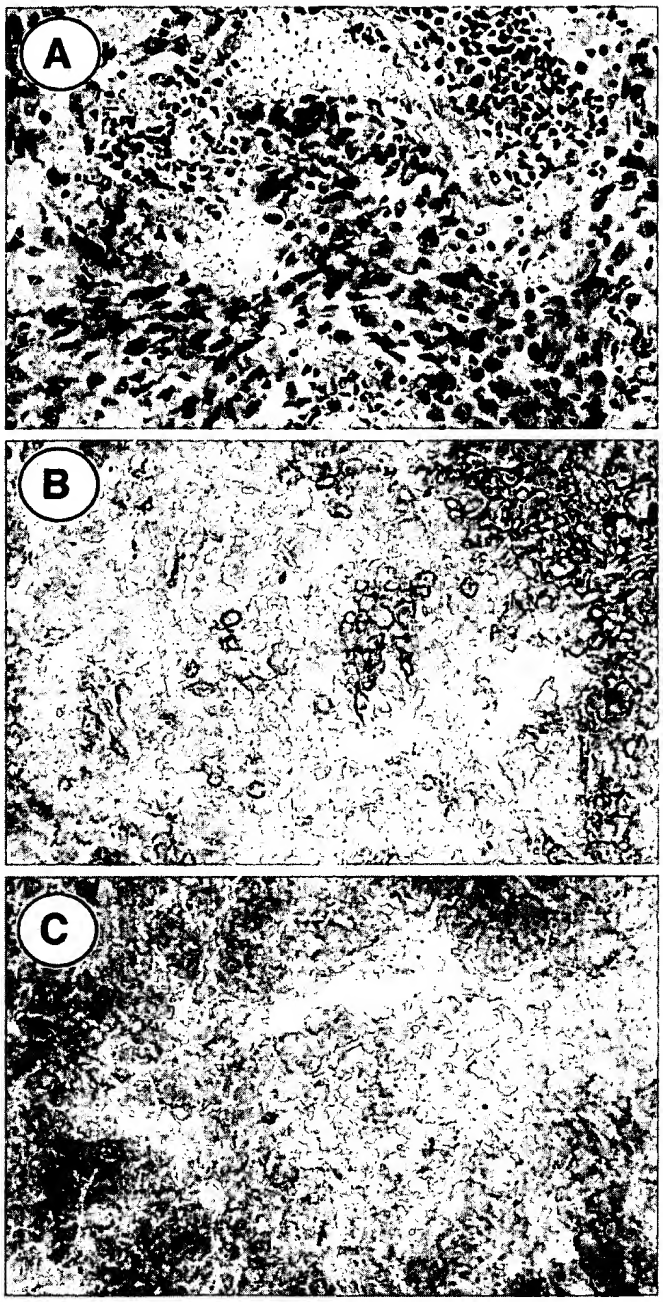

Fig. 2. CD95 staining on tissue sections of NPC biopsies. Photomicrographs of three cryostat sections of the biopsy of patient 2. *A*, stained with H&E. *B*, stained with anti-CD45 (Leukocyte Common Antigen), showing the distribution of tumor-infiltrating lymphocytes. *C*, anti-CD95 (UB2) which stains membranes of malignant epithelial cells. Magnification: *A* and *B*, ×200; *C*, ×400.

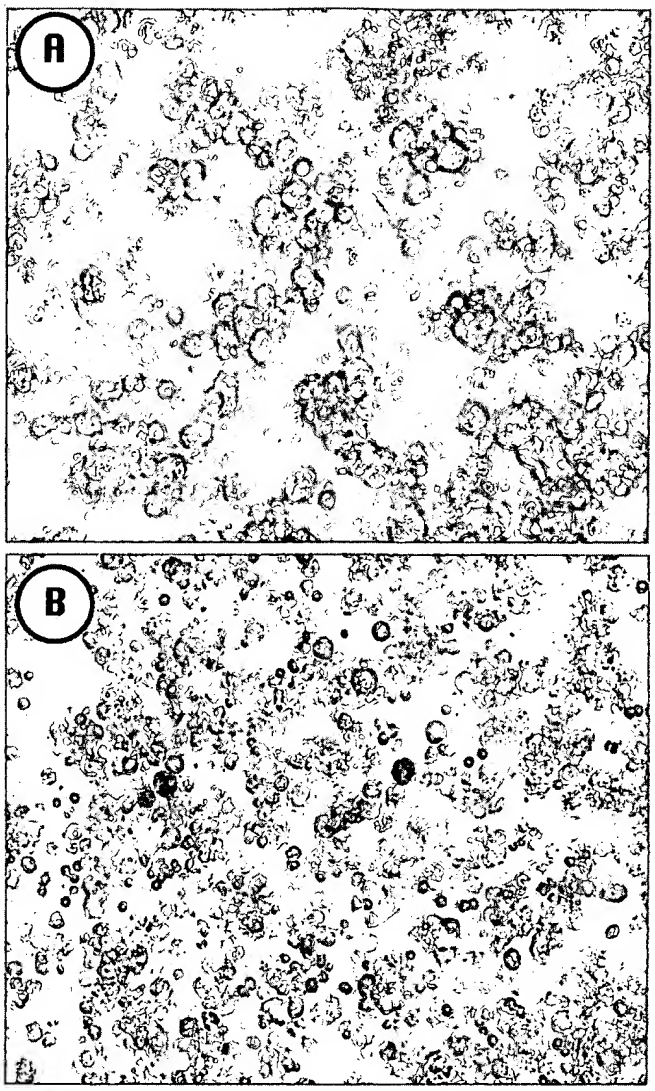

Fig. 3. Phase-contrast microscopy of C15 cells cultured *in vitro*, with or without treatment by a CD95 agonist (7C11). *A*, C15 cells (5×10^5 cells/well in a 24-well plate) incubated for 14 h with control IgM; *B*, C15 cells incubated for 14 h with the 7C11 Ab (100 ng/ml). Magnification: ×125.

CD95-mediated Apoptosis in NPC Tumor Lines. It has not been possible to derive permanent *in vitro* cell lines from the transplanted NPC tumor lines. However, cell suspensions derived from the C15 and C17 tumors can be used for short-term cultures and biological assays. This type of short-term culture was sufficient for assessment of CD95-mediated cytotoxicity that was morphologically visible within 10–12 h. Treatment of C15 and C17 cells with the 7C11 monoclonal antibody, a CD95 agonist, was highly cytotoxic (Figs. 3 and 4). This cytotoxic effect was readily detected with doses as low as 5 ng/ml. The ED_{50} was ~50 ng for C15 and 100 ng for C17 cells, in the same range as that for Jurkat cells, a classic target model for CD95 agonists. In contrast, the 7C11 monoclonal antibody had no significant effect on A431 cells obtained by nude mouse tumor dispersion (Fig. 4). To check that the toxicity of the 7C11 antibody to NPC cells was associated with typical apoptotic DNA fragmentation, agarose gel electrophoresis and oligonucleosome ELISA were performed on C15 cells incubated for 14 h with the 7C11 antibody or a control IgM (100 ng/ml; Fig. 5). Jurkat cells were processed as part of the same experiment. For Jurkat cells, DNA fragmentation and oligonucleosomes were detected only when they were treated with the CD95 agonist. In contrast, a background level of DNA fragmentation was detected with the control IgM for the C15 cells, probably due to apoptosis caused by artificial tumor cell dispersion. However, there was much more DNA and oligonucleosome fragmentation in the presence of the CD95 agonist 7C11 than with the control (more than twice as much, as measured by ELISA). Therefore, it is highly probable that the 7C11 toxicity was due to a potent and rapid apoptotic process.

CD40-mediated Increase in NPC Cell Survival. CD95 was expressed strongly on NPC cells and was extremely efficient at signaling apoptosis. We therefore investigated mechanisms that might protect NPC cells within the tumor microenvironment. Protection by CD40 activation was one attractive hypothesis, because lymphocytes infiltrating NPC consistently produce CD154, the CD40 ligand (26). To

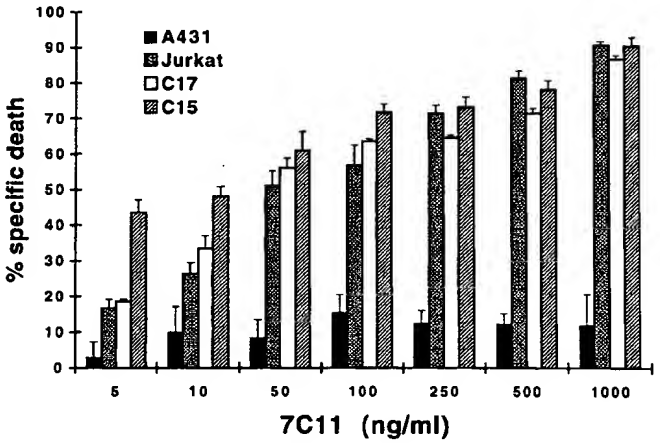

Fig. 4. Assessment of the cytotoxicity of a CD95 agonist (7C11) to the C15 and C17 cells. Viable NPC cells were counted by trypan blue dye exclusion. The data are representative of three independent experiments and the values are presented as the mean of triplicate determinations; *bars*, SD.

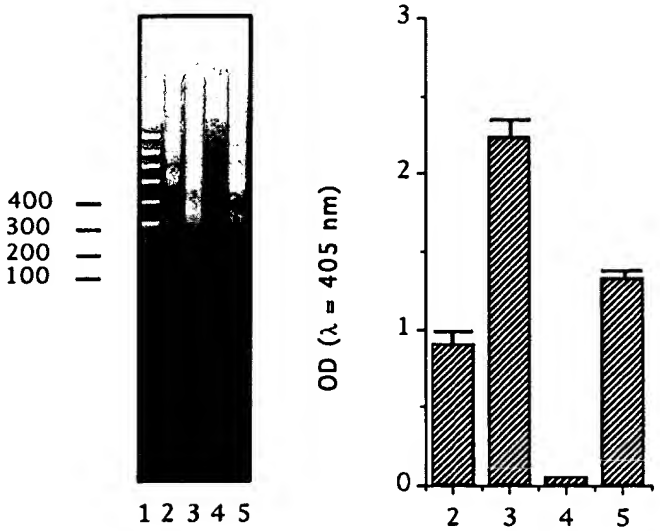

Fig. 5. Assessment of DNA fragmentation in C15 cells treated with a CD95 agonist (7C11). *Left panel*, agarose gel separation of apoptotic DNA fragments. *Right panel*, detection of oligonucleosomes by an ELISA (absorbance of the peroxidase substrate was read at 405 nm); the values are presented as the mean of triplicate determinations; *bars*, SD. *Lane 1*, DNA molecular weight markers; *Lane 2* and *column 2*, C15 cells (5×10^5/well in a 24-well plate) in short-term culture for 14 h with control IgM; *Lane 3* and *column 3*, C15 cells in short-term culture for 14 h with the CD95 agonist, 7C11 (100 ng/ml); *Lane 4* and *column 4*, Jurkat cells incubated in the same conditions with control IgM; *Lane 5* and *column 5*, Jurkat cells incubated with the 7C11 antibody (100 ng/ml).

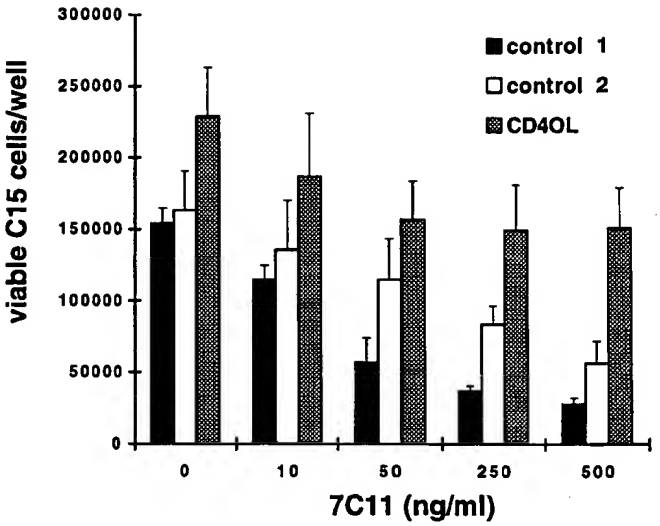

Fig. 6. Protection against Fas-mediated apoptosis by engagement of CD40. Assessment of viable NPC cells. CD40 stimulation was provided by co-cultivation with transfected murine L cells expressing the CD40 ligand (CD154). Viable C15 cells were identified among co-cultivated cells by flow cytometry analysis based on their positive HLA I staining (to test their human origin) and activation of intracellular FDA (to test their viability). *Y*-axis values are the number of viable C15 cells/well in 24-well plates. This histogram was constructed from the mean values obtained from three independent experiments. *Control 1*, C15 cells incubated without control or stimulating cells (5×10^5 cells/well); *control 2*, C15 cells incubated with nontransfected L cells (5×10^5 C15 cells + 2.5×10^5 L cells/well); *CD40L*, C15 cells incubated with L cells producing CD154 (same ratio of C15 and L cells).

test this hypothesis, we stimulated CD40 on C15 cells with transfected murine L cells having intense artificial expression of CD154. C15 and murine L cells producing CD154 were mixed, in a proportion of 2 to 1. They were incubated for 6–8 h, and the 7C11 antibody was then added for 10–14 h. Viable C15 cells were counted using a procedure based on flow cytometry analysis (Fig. 6). A much higher proportion of NPC cells survived if they were cocultivated with CD154-positive L cells prior to CD95 stimulation. Control L cells also had a nonspecific protective effect, but it was much weaker than the CD40-specific effect. With a maximum dose of CD95 agonist (500 ng/ml), there were almost three times as many viable cells if cells were mixed with CD154-producing cells rather than with control L cells. A small but consistent increase in NPC cell survival due to CD154-positive L cells was also observed in basal conditions in the absence of CD95 stimulation. Additional flow cytometry experiments were performed to confirm that the increased number of surviving NPC cells was due to a decrease in the number of apoptotic cells. Apoptotic C15 cells were identified directly by the uptake of YO-PRO-1, a nucleic acid stain that penetrates apoptotic cells even when they are still viable (28, 29). After an 8-h incubation with 250 ng/ml CD95 agonist, the fraction of viable C15 cells that was YO-PRO-1-positive was significantly lower when the cells were cocultivated with murine cells expressing CD154 (36%) compared with coculture with murine control cells (54%) or C15 cells alone (74%; Fig. 7). This is consistent with the data obtained in the previous experiment (Fig. 6). In contrast, in the absence of the CD95 agonist, the protective effect of CD40 stimulation was less clear than with the NPC cell survival assay. This is probably due to the fact that this assay recapitulates a difference in the rate of apoptosis over a longer period of time and is therefore more sensitive.

Detection of Bcl-2 and Bcl-x in NPC Tumor Lines. High concentrations of the Bcl-2 protein have been reported in about 80% of NPCs (31). Depending on the cell type, Bcl-2 and Bcl-x may interfere with CD95-mediated apoptosis (32). Therefore, we investigated the status of both proteins in our NPC tumor lines (Fig. 8). Bcl-2 was readily detected by Western blotting in C17 and C18 tumors. It was also detected, but at a low level, in the C15 tumor. The M_r 26,000 large form of Bcl-x (Bcl-x_L) was abundant in all three tumors. The amounts of Bcl-2 and Bcl-x were similar in C15 and C17 cells after tumor dissociation and 18 h of short-term culture; the amount of Bcl-x was not increased by CD40 stimulation (data not shown).

DISCUSSION

According to many reports, the level of CD95 expression is often lower in carcinoma cells than in their nonmalignant counterparts. This has been demonstrated clearly for malignant cells from colon, breast, esophagus, and cutaneous basal carcinomas (33–37). Not surprisingly, low levels or lack of CD95 cell surface expression are generally associated with a phenotype of resistance to CD95-mediated apoptosis

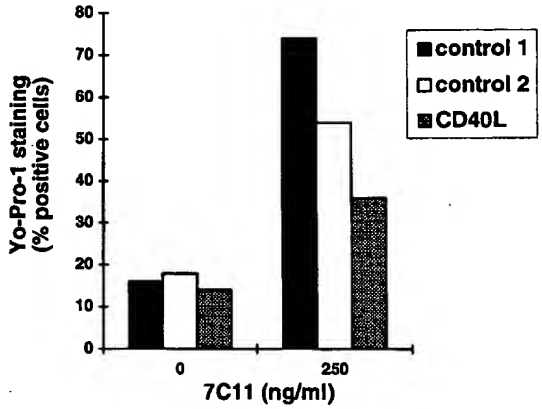

Fig. 7. Protection against Fas-mediated apoptosis by engagement of CD40. Assessment of apoptotic NPC cells. As in Fig. 6, CD40 stimulation was provided by co-cultivation with transfected murine L cells expressing the CD40 ligand. Apoptotic C15 cells were identified by flow cytometry analysis based on the uptake of YO-PRO-1, a fluorescent nucleic acid stain. Background YO-PRO-1 staining was determined on a suspension of viable L cells processed in the same experiment. *Y*-axis values are percentages of YO-PRO-1-positive cells among all cells gated out of HLA I-negative staining, reduced forward scatter, and strong side scatter (to eliminate murine cells and dead cells). This is one of three similar experiments. *Control 1*, C15 cells incubated without control or stimulating cells (5×10^5 cells/well); *control 2*, C15 cells incubated with nontransfected L cells (5×10^5 C15 cells + 2.5×10^5 L cells/well); *CD40L*, C15 cells incubated with L cells producing CD154 (same ratio of C15 and L cells).

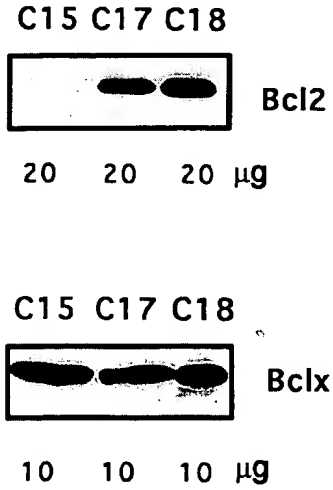

Fig. 8. Bcl-2 and Bcl-x synthesis in NPC tumor lines. The polyclonal antibody used to detect *Bcl-x* recognized both the large and the small forms of the protein. Only the large form (Bcl-x_L) was detected. On a longer exposure, a faint *Bcl-2* band was detected in *C15* material.

(34). However, resistance to CD95-mediated apoptosis is also observed frequently in carcinoma cells that have high levels of CD95 expression; such cells include prostatic, pancreatic, and some colonic carcinoma cells (38–40). In most cases, the molecular basis of this resistance is unclear. For example, the resistance of prostatic carcinoma cell lines does not correlate with the expression of Bcl-2, Bak, and Bcl-x (38).

Regardless of the mechanisms involved, the consistency of the alterations affecting the CD95 pathway suggests that these changes are important elements of tumor progression in epithelial malignancies. In this regard, EBV-positive malignant NPC cells seem to have a special status. On the basis of our present results, they appear to constitutively produce large amounts of the CD95 receptor and to remain highly susceptible to CD95-mediated apoptosis. Thus, NPC cells are probably not selected for intrinsic alterations of the CD95 receptor and its signaling pathway during tumor progression. This may be in connection with the fact that they are protected for a long time against CD95-mediated apoptosis by factors produced in the tumor microenvironment. The CD40 ligand, CD154, which is produced consistently *in situ* by tumor- infiltrating lymphocytes, is probably one such factor (26).

The functions of the CD40 receptor and its ligand have been investigated mostly in B lymphocytes. The interaction of the CD40 ligand on T cells with the CD40 receptor on B cells leads to the clonal expansion of antigen-responsive B cells and allows them to escape CD95-mediated apoptosis (23). The CD40/CD154 system has long been suspected to have a positive role in NPC tumor growth (26). However, this notion apparently conflicted with data obtained *in vitro* with non-NPC epithelial cells. CD40 stimulation has been reported to inhibit proliferation of both normal keratinocytes and several non-NPC carcinoma cell lines (41, 42). In a bladder carcinoma cell line, EJ, CD40 stimulation even potentiated the cytotoxicity of an anti-CD95 antibody (42). In contrast, we found that CD40-ligand activation protected C15 cells against CD95-mediated apoptosis. Moreover, in one of our assays, stimulation of CD40 also appeared to protect C15 cells against the background apoptosis that occurred spontaneously after tumor cell dispersion (Fig. 6). Preliminary data showed that the C17 tumor line was also protected against CD95-mediated apoptosis by stimulation of CD40 (data not shown). This is the first demonstration of an antiapoptotic effect mediated by CD40 in epithelial cells. The differences in results obtained with non-NPC cell lines, especially the EJ carcinoma, are probably due to differences in cell lineage and stage of maturation. There was no significant proliferation of NPC cells in our experimental system; therefore, we cannot exclude the possibility that stimulation of CD40 inhibits the proliferation of NPC cells. Even if this is true, the anti-apoptotic effect mediated by CD40 may favor tumor growth on the long term, despite a slower rate of proliferation. Future investigations should aim to identify other factors, such as growth factors and extracellular matrix components, that probably combine *in vivo* with the CD40 ligand to increase both cell survival and proliferation synergistically.

Efforts should also be made to determine the mechanism of the anti-apoptotic effect of CD40 stimulation. In some lymphoid cell lines, CD40 stimulation increases Bcl-x expression (43, 44). However, large amounts of Bcl-x were present in C15 and C17 cells in basal conditions, and the amount of Bcl-x was not increased by CD40 stimulation (Fig. 8 and data not shown). Other proteins thought to be involved in the control of apoptosis have been reported to be up-regulated in epithelial cells by CD40 overexpression or ligand activation: the A20 anti-apoptotic protein, the EGF receptor, and interleukin 6 (45–47). These molecules are also up-regulated by the EBV-encoded LMP1, which is expressed constitutively in C15 cells (45, 46). CD40 stimulation may act in synergy with LMP1 signals to increase the production of one or more of these molecules to provide optimal protection. Alternatively, other effector molecules might be involved in the antiapoptotic effect of CD40 stimulation in NPC cells. Their identification would be of major interest.

ACKNOWLEDGMENTS

We thank Yann Lécluse for technical assistance with flow cytometry analysis and Francine Brière (Schering-Plough, Dardilly, France) for the generous gift of CD40L L cells.

REFERENCES

1. Fahraeus, R., Fu, H. L., Ernberg, I., Finke, J., Rowe, M., Klein, G., Falk, K., Nilsson, E., Yadav, M., Busson, P., Tursz, T., and Kallin, B. Expression of Epstein-Barr virus-encoded proteins in nasopharyngeal carcinoma. Int. J. Cancer, *42:* 329–338, 1988.
2. Fries, K. L., Sculley, T. B., Webster-Cyriaque, J., Rajadurai, P., Sadler, R. H., and Raab-Traub, N. Identification of a novel protein encoded by the *Bam*HI A region of the Epstein-Barr virus. J. Virol., *71:* 2765–2771, 1997.
3. Lo, K. W., Tsao, S. W., Leung, S. D., Choi, P. H. K., Lee, J. C. K., and Huang, D. P. Detailed deletion mapping on the short arm of chromosome 3 in nasopharyngeal carcinomas. Int. J. Oncol., *4:* 1359–1364, 1994.
4. Lo, K. W., Cheung, S. T., Leung, S. F., van Hasselt, A., Tsang, Y. S., Mak, K. F., Chung, Y. F., Woo, J. K., Lee, J. C., and Huang, D. P. Hypermethylation of the p16 gene in nasopharyngeal carcinoma. Cancer Res., *56:* 2721–2725, 1996.
5. Effert, P., McCoy, R., Abdel-Hamid, M., Flynn, K., Zhang, Q., Busson, P., Tursz, T., Liu, E., and Raab-Traub, N. Alterations of the p53 gene in nasopharyngeal carcinoma. J. Virol., *66:* 3768–3775, 1992.
6. Ferradini, L., Miescher, S., Stoek, M., Busson, P., Barras, C., Cerf-Bensussan, N., Lipinski, M., Von Fliedner, V., and Tursz, T. Cytotoxic potential despite impaired activation pathways in T lymphocytes infiltrating nasopharyngeal carcinoma. Int. J. Cancer, *47:* 362–370, 1991.
7. Busson, P., Braham, K., Ganem, G., Thomas, F., Lipinski, M., Grausz, D., Wakasugi, H., and Tursz, T. Epstein-Barr virus-containing epithelial cells from nasopharyngeal carcinoma produce interleukin 1α. Proc. Natl. Acad. Sci. USA, *84:* 6262–6266, 1987.
8. Busson, P., Ganem, G., Flores, P., Mugneret, F., Clausse, B., Caillou, B., Braham, K., Wakasugi, H., Lipinski, M., and Tursz, T. Establishment and characterization of three transplantable EBV-containing nasopharyngeal carcinoma tumors. Int. J. Cancer, *42:* 599–606, 1988.
9. Busson, P., Zhang, Q., Guillon, J. M., Gregory, C. D., Young, L. S., Clausse, B., Lipinski, M., Rickinson, A. B., and Tursz, T. Elevated expression of ICAM1 (CD54) and minimal expression of LFA3 (CD58) in Epstein-Barr-virus-positive nasopharyngeal carcinoma cells. Int. J. Cancer, *50:* 863–867, 1992.
10. Al-Sarraf, M., and McLaughlin, P. W. Nasopharynx carcinoma: choice of treatment. Int. J. Radiat. Oncol. Biol. Phys., *33:* 761–763, 1995.
11. Neyts, J., Sadler, R., De Clercq, E., Raab-Traub, N., and Pagano, J. S. The antiviral agent cidofovir {(*S*)-1-(3-hydroxy-2-phosphonyl-methoxypropyl) cytosine} has pronounced activity against nasopharyngeal carcinoma grown in nude mice. Cancer Res., *58:* 384–388, 1998.
12. Crawford, D. H., Achong, B. G., Teich, N. M., Finerty, S., Thompson, J. L., Epstein, M. A., and Giovanella, B. C. Identification of murine endogenous xenotropic retrovirus in cultured multicellular tumour spheroids from nude-mouse-passaged nasopharyngeal carcinoma. Int. J. Cancer, *23:* 1–7, 1979.
13. Trauth, B. C., Klas, C., Peters, A. M., Matzku, S., Moller, P., Falk, W., Debatin, K. M., and Krammer, P. H. Monoclonal antibody-mediated tumor regression by induction of apoptosis. Science (Washington, DC), *245:* 301–305, 1989.
14. Herr, I., Wilhelm, D., Bohler, T., Angel, P., and Debatin, K. M. Activation of CD95 (APO-1/Fas) signaling by ceramide mediates cancer therapy-induced apoptosis. EMBO J., *16:* 6200–6208, 1997.
15. Nagata, S., and Golstein, P. The Fas Death Factor. Science (Washington, DC), *267:* 1449–1456, 1995.
16. Fergusson, T. A., and Griffith, T. S. A vision of cell death: insights into immune privilege. Immunol. Rev., *156:* 167–184, 1997.
17. French, L. E., Hahne, M., Viard, I., Radlgruber, G., Zanone, R., Becker, K., Muller, C., and Tschopp, J. Fas and Fas ligand in embryos and adult mice: ligand expression in several immune-privileged tissues and coexpression in adult tissues characterized by apoptotic cell turnover. J. Cell Biol., *133:* 335–343, 1996.
18. Möller, P., Walczak, H., Riedl, S., Sträter, J., and Krammer, P. H. Paneth cells express high levels of CD95 ligand transcripts. A unique property among gastrointestinal epithelia. Am. J. Pathol., *149:* 9–13, 1996.
19. Suzuki, A., Enari, M., Eguchi, Y., Matsuzawa, A., Nagata, S., Tsujimoto, Y., and Iguchi, T. Involvement of Fas in regression of vaginal epithelia after ovariectomy and during an estrous cycle. EMBO J., *15:* 211–215, 1996.
20. Yue, T. L., Ma, X. L., Wang, X., Romanic, A. M., Liu, G. L., Louden, C., Gu, J. L., Kumar, S., Poste, G., Ruffolo, R. R., Jr., and Feuerstein, G. Z. Possible involvement of stress-activated protein kinase signaling pathway and Fas receptor expression in prevention of ischemia/reperfusion-induced cardiomyocyte apoptosis by carvedilol. Circ. Res., *82:* 166–174, 1998.
21. Stamenkovic, I., Clark, E. A., and Seed, B. A B-lymphocyte activation molecule related to the nerve growth factor receptor and induced by cytokines in carcinomas. EMBO J., *8:* 1403–1410, 1989.

22. Mach, F., Schonbeck, U., Sukhova, G. K., Bourcier, T., Bonnefoy, J. Y., Pober, J. S., and Libby, P. Functional CD40 ligand is expressed on human vascular endothelial cells, smooth muscle cells, and macrophages: implications for CD40-CD40 ligand signaling in atherosclerosis. Proc. Natl. Acad. Sci. USA, *94:* 1931–1936, 1997.
23. Lagresle, C., Mondière, P., Bella, C., Krammer, P. H., and Defrance, T. Concurrent engagement of CD40 and the antigen receptor protects naive and memory human B cells from Apo-1/Fas-mediated apoptosis. J. Exp. Med., *183:* 1377–1388, 1996.
24. Björck, P., Banchereau, J., and Flores-Romo, L. CD40 ligation counteracts Fas-induced apoptosis of human dendritic cells. Int. Immunol., *9:* 365–372, 1997.
25. Young, L. S., Dawson, C. W., Brown, K. W., and Rickinson, A. B. Identification of a human epithelial cell surface protein sharing an epitope with the C3d/Epstein-Barr virus receptor molecule of B lymphocytes. Int. J. Cancer, *43:* 786–794, 1989.
26. Agathanggelou, A., Niedobitek, G., Chen, R., Nicholls, J., Yin, W., and Young, L. S. Expression of immune regulatory molecules in Epstein-Barr virus-associated nasopharyngeal carcinomas with prominent lymphoid stroma. Evidence for a functional interaction between epithelial tumor cells and infiltrating lymphoid cells. Am. J. Pathol., *147:* 1152–1160, 1995.
27. Segal-Bendjirdjian, E., and Jacquemin-Sablon, A. Cisplatin resistance in a murine leukemia cell line is associated with a defective apoptotic process. Exp. Cell Res., *218:* 201–212, 1995.
28. Garrone P., Neidhardt, E. M., Galibert, L. C., and Banchereau, J. Fas ligation induces apoptosis of CD40-activated human B lymphocytes. J. Exp. Med., *182:* 265–271.
29. Estaquier, J., Idziorek, T., Zou, W., Emilie, D., Farber, C. M., Bourez, J. M., and Ameisen, J. C. T Helper type 1/T helper type 2 cytokines and T cell death: preventive effect of interleukin 12 on activation-induced and CD95 (Fas/Apo-1)-mediated apoptosis of $CD4^+$ T cells from human immunodeficiency virus-infected persons. J. Exp. Med., *182:* 1759–1767, 1995.
30. Daly, J. M., Jannot, C. B., Beerli, R. R., Graus-Porta Diana, Maurer, F. G., and Hynes, N. E. Neu differentiation factor induced erbB2 down-regulation and apoptosis of erbB2-overexpressing breast tumor cells. Cancer Res., *57:* 3804–3811, 1997.
31. Lu, Q. L., Elia, G., Lucas, S., and Thomas, J. A. *Bcl-2* proto-oncogene expression in Epstein-Barr-virus-associated nasopharyngeal carcinoma. Int. J. Cancer, *53:* 29–35, 1993.
32. Scaffidi, C ., Fulda, S., Srinivasan, A., Friesen, C., Li, F., Tomaselli, K. J., Debatin, K. M., Krammer, P. H., and Peter, M. E. Two CD95 (APO-1/Fas) signaling pathways. EMBO J., *17:* 1675–1687, 1998.
33. Möller, P., Koretz, K., Leithäuser, F., Brüderlein, S., Henne, C., Quentmeier, A., and Krammer, P. H. Expression of Apo-1 (CD95), a member of the NGF/TNF receptor superfamily, in normal and neoplastic colon epithelium. Int. J. Cancer, *57:* 371–377, 1994.
34. Keane, M. M., Ettenberg, S. A., Lowrey, G. A., Russell, E. K., and Lipkowitz, S. Fas expression and function in normal and malignant breast cell lines. Cancer Res., *56:* 4791–4798, 1996.
35. Hughes, S. J., Nambu, Y., Soldes, O. S., Hamstra, D., Rehemtulla, A., Iannettoni, M. D., Orringer, M. B., and Beer, D. G. Fas/APO-1 (CD95) is not translocated to the cell membrane in esophageal adenocarcinoma. Cancer Res., *57:* 5571–5578, 1997.
36. Gratas, C., Tohma, Y., Barnas, C., Taniere, P., Hainaut, P., and Ohgaki, H. Up-regulation of Fas (APO-1/CD95) ligand and down-regulation of Fas expression in human esophageal cancer. Cancer Res., *58:* 2057–2062, 1998.
37. Gutierrez-Steil, C., Wrone-Smith, T., Sun, X., Krueger, J. G., Coven, T., and Nickoloff, B. J. Sunlight-induced basal cell carcinoma tumor cells and ultraviolet-B-irradiated psoriatic plaques express Fas ligand (CD95L). J. Clin. Invest., *101:* 33–39, 1998.
38. Rokhlin, O. W., Bishop, G. A., Hostager, B. S., Waldschmidt, T. J., Sidorenko, S. P., Pavloff, N., Kiefer, M. C., Umansky, S. R., Glover, R. A., and Cohen, M. B. Fas-mediated apoptosis in human prostatic carcinoma cell lines. Cancer Res., *57:* 1758–1768, 1997.
39. Ungefroren, H., Voss, M., Jansen, M., Roeder, C., Henne-Bruns, D., Kremer, B., and Kalthoff, H. Human pancreatic adenocarcinomas express Fas and Fas ligand yet are resistant to Fas-mediated apoptosis. Cancer Res., *58:* 1741–1749, 1998.
40. Yanagisawa, J., Takahashi, M., Kanki, H., Yano-Yanagisawa, H., Tazunoki, T., Sawa, E., Nishitoba, T., Kamishohara, M., Kobayashi, E., Kataoka, S., and Sato, T. The molecular interaction of Fas and FAP-1. A tripeptide blocker of human Fas interaction with FAP-1 promotes Fas-induced apoptosis. J. Biol. Chem., *272:* 8539–8545, 1997.
41. Péguet-Navarro, J., Dalbiez-Gauthier, C., Moulon, C., Berthier, O., Reano, A., Gaucherand, M., Banchereau, J., Rousset, F., and Schmitt, D. CD40 ligation of human keratinocytes inhibits their proliferation and induces their differentiation. J. Immunol., *158:* 144–152, 1997.
42. Eliopoulos, A. G., Dawson, C. W., Mosialos, G., Floettmann, J. E., Rowe, M., Armitage, R. J., Dawson, J., Zapata, J. M., Kerr, D. J., Wakelam, M. J. O., Reed, J. C., Kieff, E., and Young, L. S. CD40-induced growth inhibition in epithelial cells is mimicked by Epstein-Barr virus-encoded LMP1: involvement of TRAF3 as a common mediator. Oncogene, *13:* 2243–2254, 1996.
43. Choi, M. S., Boise, L. H., Gottschalk, A. R., Quintans, J., Thompson, C. B., and Klaus, G. G. The role of bcl-XL in CD40-mediated rescue from anti-mu-induced apoptosis in WEHI-231 B lymphoma cells. Eur. J. Immunol., *25:* 1352–1357, 1995.
44. Ishida, T., Kobayashi, N., Tojo, T., Ishida, S., Yamamoto, T., and Inoue, J. CD40 signaling-mediated induction of Bcl-XL, Cdk4, and Cdk6. Implication of their cooperation in selective B cell growth. J. Immunol., *155:* 5527–5535, 1995.
45. Miller, W. E., Mosialos, G., Kieff, E., and Raab-Traub, N. Epstein-Barr virus LMP1 induction of the epidermal growth factor receptor is mediated through a TRAF signaling pathway distinct from NF- κB activation. J. Virol., *71:* 586–594, 1997.
46. Eliopoulos, A. G., Stack, M., Dawson, C. W., Kaye, K. M., Hodgkin, L., Sihota, S., Rowe, M., and Young, L. S. Epstein-Barr virus-encoded LMP1, and CD40 mediate IL-6 production in epithelial cells via an NF-κB pathway involving TNF receptor-associated factors. Oncogene, *14:* 2899–2916, 1997.
47. Chauhan, D., Kharbanda, S., Ogata, A., Urashima, M., Teoh, G., Robertson, M., Kufe, D. W., and Anderson, K. C. Interleukin-6 inhibits Fas-induced apoptosis and stress-activated protein kinase activation in multiple myeloma cells. Blood, *89:* 227–234, 1997.

hydrogen butanedioate and 1,2,2,6,6-tetramethyl-4-piperidinyl 2-methyl-2-propenoate *[180641-09-2]*, acrylic vinyl chloride-based resin emulsions contg. reactive emulsifiers and reactive light stabilizers for coatings, 125: *pr* P 169593f
SX 1159
polymer with chloroethene, 2-ethylhexyl 2-propenoate and 2,2,6,6-tetramethyl-4-piperidinyl 2-methyl-2-propenoate *[180641-08-1]*, acrylic vinyl chloride-based resin emulsions contg. reactive emulsifiers and reactive light stabilizers for coatings, 125: *pr* P 169593f
polymer with 2-ethylhexyl 2-propenoate, 1,6-hexanediyl di-2-propenoate, 2-hydroxypropyl 2-propenoate and 2,2,6,6-tetramethyl-4-piperidinyl 2-methyl-2-propenoate *[180641-10-5]*, acrylic vinyl chloride-based resin emulsions contg. reactive emulsifiers and reactive light stabilizers for coatings, 125: *pr* P 169593f
SX 9-0220 *[180983-84-0]*
phosphorescent humidifiers and vaporizers, 125: P 207978v
SX 6020B *[138362-14-8]*
flame retardants, for drying oil-modified aldehyde-phenol copolymers, 116: P 42621x
SX 310F *[175206-10-7]*
coating; for printing interior material fabrics with good print sharpness and color build-up properties, 124: P 263321s
SXM 18 *[162122-83-0]*
degrdn. of multiply epoxy/graphite fiber composites induced by space environment, 122: 215760w
204SXZL386 *[159704-93-5]*
membrane; current dependence of the electro-osmotic permeability in ion-exchange membranes, 122: 17723y
SY 6 *[148465-50-3]*
resonators from, synchrotron beam acceleration in relation to, 119: 35764m
SY 8 *[173717-83-4]*
adhesive; adhesive effect on interlaminar property of ARALL, 124: 152429p
SY 14 (adhesive) *[173717-84-5]*
adhesive; adhesive effect on interlaminar property of ARALL, 124: 152429p
influence of exposure state of adhesives on results of wet-heat aging, 125: 223694e
SY 17 *[142583-75-3]*
finishing agents, for rabbit hair, 117: P 50691f
SY 26 *[145240-23-5]*
adhesives, for boron-iron-neodymium magnets, curing and mech. properties of, 118: 103985j
SY 244 *[135229-98-0]*
photog. film contg., 117: P 160784w
SYBR 14 *[166799-45-7]*
viability assessment of mammalian sperm by fluorescent staining with SYBR-14 and propidium iodide, 123: 137819b
SYBR Green I *[163795-75-3]*
anal. of double-stranded DNA by capillary electrophoresis with laser-induced fluorescence detection using the monomeric dye SYBR Green I, 124: 1747q
increase in detection sensitivity of viral DNA after polymerase chain reaction by SYBR Green I relative to ethidium bromide DNA staining, 123: 219496h
nonradioactive detection of hypervariable simple sequence repeats in short polyacrylamide gels which are stained with SYBR™ Green to visualize and photograph bands on an UV transilluminator, 123: 219451q
quant. detection of reverse transcriptase-PCR products by a sensitive DNA stain, 123: 2070e
a quant. method of detg. initial amts. of DNA by polymerase chain reaction cycle titrn. using digital imaging and a novel DNA stain, 125: 27092t
SYBR Green II *[172827-25-7]*
a fluorometric assay for the quantification of RNA in soln. with nanogram sensitivity, 124: 111410g
in nonradioactive single-strand conformation polymorphism anal. with application for mutation detection in a mixed population of cells, 124: 308815z
SYBR Green II stain for RNA requires no destaining for use in formaldehyde gels, 125: 29364g
Sybron $(Pr)_3N$ *[166516-46-7]*
anion exchanger contg. tripropylamine; distribution of 14 elements from two solns. simulating Hanford HLW tank 102-SY on anion exchangers, 123: 125352f
Sybron Stainfree *[143477-48-9]*
dye resists, for printing of nylon carpets in multishades, 117: P 132855b
stain repellent compns. contg.; method and compn. for increasing repellency on carpet and carpet yarn, 125: P 117327c
stain resist compns. contg. alkene-maleic anhydride copolymer and, for polyamide textiles, 121: P 136175k
SY 24C *[181788-97-6]*
influence of exposure state of adhesives on results of wet-heat aging, 125: 223694e
SY 102C *[158854-55-8]*
acrylic polymer; manuf. of flocked plastic moldings by adding fibers in plastics, 121: P 257394q
Sycar *[161184-17-7]*
characteristics of low-loss, low-dielec. const. and high-glass-temp. polycarbosilane for use in high-frequency digital device interconnection, 123: 258972e
encapsulants, for integrated circuits, 119: 251536e
high thermal conductance liq. encapsulants for direct chip attach, 125: 319642s
potting compns., for integrated circuits, 119: 251535y
silicon-carbon resin technol. for high-performance printed wiring board applications, 123: 230417d
SY-Coat E 6 *[182176-74-6]*
impact-resistent fiber-reinforced plastic laminates, 125: P 249829c
SY-D 4 *[181788-98-7]*
influence of exposure state of adhesives on results of wet-heat aging, 125: 223694e
SY-D 9 *[181788-99-8]*
influence of exposure state of adhesives on results of wet-heat aging, 125: 223694e
Sydplast LPLM 15 *[142902-01-0]*
physicochem. and mech. properties of, 117: 91334k
Sydplast LPLM 8016 *[142902-02-1]*
physicochem. and mech. properties of, 117: 91334k
SY-Glyster ML 800 *[146702-56-9]*
foaming alc. beverage compns. contg., 118: P 190474h
in prepn. of foam beverages, 118: P 168067f
SY-Glyster PO 310 *[179800-51-2]*
deep-frying oils contg. emulsifiers, sugar alcs., and polyglycerin, 125: P 141183y
SYK *[67763-78-4]*
fuller's earth, adsorbent; cleaning of electronic components, 123: P 148089q
Sylobloc 42 *[170137-42-5]*
antiblocking agent; oriented HDPE films with skin layers for food packaging contg., 123: P 316241d
Sylobloc 45 *[179733-77-8]*
water and surfaces treatment with compns. or paints as molluscicides, 125: P 123188z
Syl-off 7046 *[158164-19-3]*
release agent, for manufg. adhesive tape carrying hologram as security device for goods, 121: P 232648a
Sylophobic 100 *[181591-88-8]*
reversible thermal recording material having hydrophobic silica-contg. polymer protective layer, 125: P 234459h
Sylophobic 505 *[172672-67-2]*
propylene polymer compns. contg. surface-treated silica antiblocking agents and phosphorus-phenol antioxidants for manuf. of scratch-resistant films, 124: P 89499u
Sylophobic 507 *[177345-97-0]*
masterbatching polyolefin and inorg. particles of particular size for producing blocking-resistant polyolefin film, 125: P 12477y
Sylophobic 704 *[174794-94-6]*
coatings for reducing fluid drag on surfaces, 124: P 235051k
Sylothix 52 *[179393-77-2]*
reinforcing agents; tin-free, fiber-reinforced antifouling paint compn., 125: P 117587n
Sylothix 53 *[179393-78-3]*
reinforcing agents; tin-free, fiber-reinforced antifouling paint compn., 125: P 117587n
Sylvania 1-1 *[153190-23-9]*
characteristics of luminescent lamps with, 120: 147677f
Sylvania 2-2 *[153190-24-0]*
strontium fluoroborate activated with europium, 120: 147677f
Sylvania 50 *[180473-20-5]*
phosphor; cyanoethylated acrylic monomer-fluoropolymer graft copolymers, their manuf., and electroluminescent devices, 125: P 180943r
Sylvania 246 *[105522-01-8]*
fluorescent lamps with high color-rendering and high brightness using metameric blends, 122: P 67924k
fluorescent lamp with improved color rendering index and brightness, 122: P 67874u
Sylvania 290 *[159814-38-7]*
lead- and manganese-activated, fluorescent lamps with high color-rendering and high brightness using metameric blends, 122: P 67924k
Sylvania 723 *[139691-14-8]*
dispersion-type electroluminescent devices from, 118: P 157552j
electroluminescent devices from, with org. binders, 116: P 139750b
Sylvania 2194 *[159814-39-8]*
fluorescent lamps with high color-rendering and high brightness using metameric blends, 122: P 67924k
Sylvania 2288 *[160047-63-2]*
fluorescent lamps with high color-rendering and high brightness using metameric blends, 122: P 67924k
fluorescent lamp with improved color rendering index and brightness, 122: P 67874u
Sylvania 2293 *[159814-40-1]*
fluorescent lamps with high color-rendering and high brightness using metameric blends, 122: P 67924k
Sylvania 2345 *[159814-41-2]*
fluorescent lamps with high color-rendering and high brightness using metameric blends, 122: P 67924k
fluorescent lamp with improved color rendering index and brightness, 122: P 67874u
Sylvania 6350 *[153190-25-1]*
comparative luminescent characteristics of, 120: 147677f
Sylvania 6354 *[37224-36-5]*
comparative luminescent characteristics of, 120: 147677f
Sylvania SAE *[160047-64-3]*
fluorescent lamp with improved color rendering index and brightness, 122: P 67874u
Sylvanite *[1301-81-1]*
anal. for Te by AAS and spectrophotometry using electrodeposition preconcn., 123: 125872c
beneficiation of, clay slurries from, structural-rheol. properties of, improvement of, by lignosulfonate treatment, 121: 90891v
compn. and origin; in hydrothermal vein ores, Detiangou gold deposit, Beijing, China, 123: 138346m
compn. of
in gold-silver telluride deposits, of alk. intrusive host rocks, of Gies, Judith Mts., Montana, 121: 87746m
compn. of
intergrowth with nagyagite, from gold-tellurium ore deposits, 120: 249376s
in kuroko type ore deposit, of Iwami mine, southwestern Japan, 116: 132931c
in porphyry copper ore deposit, of Skouries, Greece, 116: 132962p
crystal chem. implications of ^{197}Au Moessbauer study of gold-silver ditellurides, 122: 192673d
flotation, roasting and leaching of, 123: 233767d
gold detn. in, by spectrophotometry, 117: 19466n
gold-197 Moessbauer spectra of, crystallog. siting of gold in relation to, 120: 327652c
gold-197 Moessbauer spectrum of, 117: 52537j
interpretation of ^{197}Au Moessbauer study of gold-silver ditellurides, 122: 192674e
recovery from sylvanite by flotation, roasting and cyanide leaching, 123: 175396u
telluride minerals from the Detiangou gold ore deposit, Beijing, 125: 119696w
Sylvatac 295 *[113096-38-1]*
tackifier; hot-melt adhesive compn. for manuf. of disposable soft goods, 123: P 146091k
tall oil resin hot-melt jet ink compn. contg. benzoate rheol. modifiers, 122: P 317082u
Sylvatac 5N *[160338-70-5]*
hot melt adhesive compn. with improved thermal resistance, 122: P 57707c
Sylvatac 40N *[144696-98-0]*
Bu acrylate-ethylene copolymer-based hot-melt adhesive compns. applicable at lower temp., 125: P 170204m
tacking agent contg., for printed circuit board manuf., 117: P 263064r
Sylvatac R 85 *[148499-24-5]*
tackifier; removable preasure-sensitive adhesives for recyclable substrates, 123: P 11314q
tackifiers, acrylic adhesives contg., for removable labels, 119: P 29644z
Sylvatac ST 140 *[173329-44-7]*
tackifiers; acrylic adhesives contg. alkyl (meth)acrylate-vinyl copolymers, tackifiers and crosslinking agents, useful for tapes, 124: P 119713d
Sylverin *[152685-51-3]*
amino acid sequence and toxicity of, of Protonectarina sylveirae, 120: 156293e
amino acid sequence of and mast cell degranulation and histamine release induction by, 120: 102465u
of venom sac of Protonectarina sylveirae, isolation and mast cell histamine-releasing activity of, 121: P 104807b
Sylverin (reduced) *[152645-67-5]*

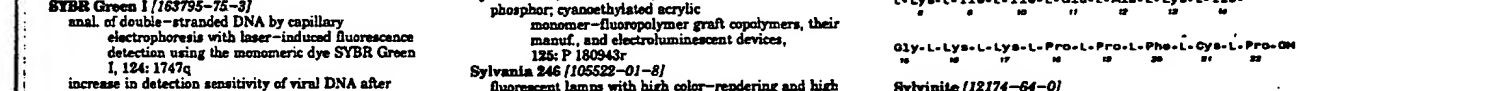

Sylvinite *[12174-64-0]*
aliph. amine-, hydrocarbonaceous extender oil-, and emulsifier-contg. aq. compns. for ore flotation, 124: P 264942g
aliph. amine-contg. aq. compns. for ore flotation, 124: P 264943h
base component, in fire extinguishing compn. contg. silica gel powd. and aluminosilicate, 120: P 248746h
beneficiation of, suspended clay-carbonate slime sepn. from brine in, 116: P 23943n
bicyclic amine adsorption on salt minerals and flotation processes, 124: 299835b
coating mixt. contg., in welding, melt splash damage prevention by, 117: P 238393q
content and distribution pattern of Au, Ag, and Pt-group metals in sylvinite from the Verkhnekama potassium ore deposit, 123: 261879k
conversion with nitrates in complex fertilizer manuf., 124: 288153b
co-prodn. of potassium sulfate and sodium sulfate from potash and hydrated sodium sulfate, 125: P 90620d
desliming of ores of, by flotation of clay-carbonate impurities with protein collector, 116: 62757s
dissoln. of ores of, for potassium chloride and sodium chloride recovery, 117: 51791a
extn. of potassium chloride from sylvinite ores by flotation using collector of acyl hydrazides, 123: P 87544k
flotation of
in brine solns., flotation modifiers for, 116: P 177134m
chloride soln. surface tension at gas boundary in relation to, 120: 138627n
polyacrylamide-CMC polycomplex in, modifying properties of, 118: 257618d
flotation of argillaceous, nonpolar reagent effect on, 121: *pr* 62066b
flotation of clay-carbonate slurries of, conditioning agent for, 121: *pr* P 137123d
of forecasting and optimization computer programs for ore prepn. and flotation processes at potash beneficiation plants of CIS., 124: 93341w
hallite mixt.; phys. interpretation of energy- and entropy-based sepn. efficiencies, 123: *pr* 61888p
magnesium-contg., potassium chloride recovery from, 119: 142208y
manuf. of potassium chloride by flotation concn. of sylvinite, 125: P 37398m
manuf. of salts by leaching of mineral deposits and cooling of resulting solns., 125: P 253178p

AL (Gene Therapy Program, University of Alabama at Birmingham, Birmingham, AL 35294-0005 USA). *Gene Ther.* 1995, 2(9), 660–8 (Eng). A major concern assocd. with the use of recombinant adenoviral vectors is that viral receptors are found on the surface of many cell types and systemic in vivo delivery of the viral vector could result in uncontrolled and widespread expression of therapeutic mols. in many tissues. To construct a cell-type specific recombinant adenoviral vector, a new binding specificity must be added to the virus, and the endogenous binding specificity of the virus must be ablated. In order to introduce a new binding specificity to recombinant adenoviral vectors, the coding sequence of a physiol. ligand, the terminal decapeptide of the gastrin releasing peptide (GRP), was placed at the 3' end of the coding sequence of the adenovirus type 5 fiber gene. The resulting fiber–GRP fusion protein was expressed using a T7 vaccinia expression system and has been shown to assemble protein trimers whose quaternary structure is indistinguishable from that of wild-type protein. The fiber–GRP fusion protein was correctly transported to the nucleus of HeLa cells immediately after synthesis. The added GRP ligand in the fiber–GRP fusion protein was accessible to binding by an anti-GRP antibody in both the monomeric and trimeric forms of the chimeric protein. These studies suggest that new cell type specificities for adenovirus binding might be introduced by genetic fusion of peptide ligands on to the carboxyl terminus of the adenovirus fiber protein.

124: 1745n **Solid-phase nested deletion: a new subcloning-less method for generating nested deletions.** Yohda, Masafumi; Kato, Nobuko; Endo, Isao (Chem. Engineering Laboratory, The Inst. Phys. and Chem. Res. (RIKEN), Wako, Japan 351-01). *DNA Res.* 1995, 2(4), 175–81 (Eng). We have developed a new subcloning-less method for generating nested deletions which we have termed Solid-Phase Nested Deletion. The basic procedure for this method is as follows. The target DNA fragment is cloned in the multiple cloning site of a cloning vector, pUC or its derivs., and amplified by PCR using a set of primers, one of which is 5'-biotinylated. The amplified DNA is partially digested by a restriction enzyme with a 4-base recognition sequence. The digested DNA is ligated with a synthetic adapter DNA. Monodiverse beads coupled with streptavidin (Dynabeads™ M-280 streptavidin) are added to the mixt. and the biotinylated DNA fragments are sepd. by applying magnetic field. The unidirectionally deleted DNA fragments are recovered by PCR from the magnetic beads, and size-fractionated by agarose gel electrophoresis. The DNA fragments are amplified by PCR and used for sequencing. We demonstrate the potential of this method using a 4878-bp EcoRI fragment of λ phage DNA.

124: 1746p **Direct detection of the expanded CAG repeat in IT15 gene for molecular diagnosis of Huntington's disease.** Mao, Yuehua; Zhou, Gang; Chen, Meijue; Ren, Zhaorui; Zeng, Yitao; Wang, Xiuying; Xu, Zhida (Shanghai Inst. Med. Genetics, Shanghai Children's Hospital, Shanghai, Peop. Rep. China 200040). *Gaojishu Tongxun* 1995, 5(5), 1–6 (Ch). We used nested PCR and denaturing polyacrylamide gel electrophoretic autoradiog. to analyze the normal and expanded alleles of the $(CAG)_n$ repeat in the IT15 gene in Chinese normal and Huntington's disease (HD) chromosomes. A total of 40 normal controls as well as 46 related members of two HD pedigrees from Xuzhou and Zhejiang, resp., were studied. The normal alleles contained approx. 16 CAG repeat, while all the HD alleles had over 40 copies of (CAG) and there was no overlap between the normal and affected alleles. The presymptomatic diagnosis of 38 family members at risk for HD disclosed that 11 subjects carried the affected alleles, which was in accordance with the pedigree investigation and clin. anal. Thus, the dynamic mutations in IT15 gene were responsible for HD in the Chinese.

124: 1747q **Analysis of double-stranded DNA by capillary electrophoresis with laser-induced fluorescence detection using the monomeric dye SYBR Green I.** Skeidsvoll, Jarle; Ueland, Per Magne (Dep. Clinical Biol., Univ. Bergen, N-5021 Bergen, Norway). *Anal. Biochem.* 1995, 231(2), 359–65 (Eng). The monomeric fluorescent dye, SYBR Green I, was investigated and compared with the dyes YO-PRO-1 and thiazole orange (TO) for their application in capillary electrophoresis (CE) with laser-induced fluorescence (LIF) detection of double-stranded DNA (dsDNA). DNA fragments were injected by hydrodynamic pressure and sepd. in a replaceable matrix of hydroxypropyl methylcellulose. For all 3 dyes, optimal concns. were established and efficient sepns. of DNA fragments ranging in size from 75 to 12216 bp were obtained. The most promising results in terms of linear detection range were achieved with SYBR Green I. At the optimal dye concn., fluorescence intensity vs. DNA concn. was linear over more than three orders of magnitude (4 pg/μl to 30 ng/μl). Limit of detection (LOD) with SYBR Green I was approx. 80 fg of dsDNA (240 zmol of a 200-bp fragment). Similar LOD was obtained with YO-PRO-1, whereas TO resulted in lower sensitivity. Precision in both fluorescence intensity and migration time was high (relative std. deviation, RSD < 3.6%; n = 10) for dsDNA fragments complexed with SYBR Green I. In conclusion, SYBR Green I is a fluorescent dye well suited for efficient sepn. and quant., sensitive, and precise detn. of dsDNA by CE-LIF.

124: 1748r **Direct automated sequencing of single λ-phage plaques by exponential amplification sequencing.** Hwang, David M.; Wang, Ruo-Xiang; Liew, Choong-Chin (Lab. Mol. Cardiol., Univ. Toronto, Toronto, ON Can.). *Anal. Biochem.* 1995, 231(2), 460–3 (Eng). We developed a method for single-step sequencing directly from individual λ-phage plaques by exponential amplification (EAS). In this report, we present results of EAS performed on single plaques from a directionally cloned human fetal heart cDNA library, and we demonstrate its potential utility to large-scale sequencing projects.

124: 1749s **Fine-mapping of shotgun template libraries; an efficient strategy for the systematic sequencing of genomic DNA.** Scholler, Patrik; Karger, Achim E.; Meier-Ewert, Sebastian; Lehrach, Hans; Delius, Hajo; Hoheisel, Joerg D. (Mol.-Genetic Genome Anal. Group, Deutsches Krebsforschungszentrum, D-69120 Heidelberg, Germany). *Nucleic Acids Res.* 1995, 23(19), 3842–9 (Eng). To test the effectiveness of ordering shotgun DNA-templates prior to sequence anal., the 450 kb left arm of yeast chromosome XII was randomly subcloned into a phagemid vector. Clones were ordered by hybridization to an av. map d. of one new insert every 125 bp and are currently used for sequencing the chromosomal fragment. An 11.5-kb overlap between the template map and a DNA fragment that had been sequenced earlier allowed an independent evaluation of the strategy's effectiveness. To this end, clones were selected from the map and tag-sequenced from either end, thus comparing the map position with the actual location within the 11.5 kb. Of 65 selected clones, taken mostly at random from a total of 423, 58 mapped on av. about a quarter of a clone length around their predicted position, with the other seven being between 0.6 and 1.5 clone length off. 75–86 Sequencing reactions on clones selected from the map would have been sufficient for completely sequencing both strands of the 11.5-kb fragment. The results demonstrate the efficacy of such template sorting, considerably assisting sequencing at relatively little cost on the mapping level.

124: 1750k **Large scale isolation of expression vector cassette by magnetic triple helix affinity capture.** Sonti, Srinivas V.; Grifor, Matthew C.; Sano, Takeshi; Narayanswami, Sandya; Bose, Arijit; Cantor, Charles R.; Kausch, Albert P. (Dep. Chem. Eng., Univ. Rhode Island, Kingston, RI 02881 USA). *Nucleic Acids Res.* 1995, 23(19), 3995–6 (Eng). A novel procedure was developed to purify DNA fragments by using the specificity of triple helix formation. The authors present a rapid method for vector cassette isolation that provdes DNA prepns. free of contaminating plasmid sequences by constructing DNA expression vectors contg. triple helix-forming seuqences which can be digested from the plasmid and isolated by incubating with biotinylated triple helix-forming oligonucleotide follwed by magnetic strepavidin sepn. Two plant expression cassettes, p538 and p539 were constructed using the homopurine/homopyrimidine triple helix forming sequence from plasmid pTC45,T-$(T\text{-}C)_{22}$ and a cauliflower mosaic virus 35S/GUS/Tr7 insert from plasmid p165.

124: 1751m **Rapid DNA preparation for 2D gel analysis of replication intermediates.** Wu, Jia-Rui; Gilbert, David M. (Dep. Biochem. Mol. Biol., SUNY Health Sci. Cent., Syracuse, NY 13210 USA). *Nucleic Acids Res.* 1995, 23(19), 3997–8 (Eng). A simplified method was developed for isolating yeast genomic DNA for two-dimensional (2D) agarose gel electrophoresis anal. from smaller no. of Saccharomyces cerevisiae yeast cells. The method can be used to prep. 20–25μg DNA from 50 mL cell culture in ~6 h. Glass beads are used to disrupt the cell walls, followed by column chromatog. on a Qiagen column. DNA eluates are pptd. with isopropanol, then collected by microcentrifugation. The Qiagen mini prepn. tip (20/G) was selected since this allows isolation of genomic DNA starting with smaller nos. of cells. The method can be scaled up to prep. larger quantities of DNA, if necessary, using larger columns.

124: 1752n **Hydroxyquinoline overcomes PCR inhibition by UV-damaged mineral oil.** Gilgen, M.; Hoefelein, C.; Luethy, J.; Huebner, Ph. (Lab. Food Chem., Inst. Biochem., Univ. Bern, 3012 Bern, Switz.). *Nucleic Acids Res.* 1995, 23(19), 4001–2 (Eng). Mineral oil, treated overnight with UV irradn., inhibits PCR reactions. The inhibition can be overcome by the antioxidans 8-hydroxyquinoline (I), thus supporting the idea that the inhibition is caused by radicals. I itself does not hamper PCR. Surprisingly, the sensitivity of PCR was slightly increased with I.

124: 1753p **A lacZ-hygromycin fusion gene and its use in a gene trap vector for marking embryonic stem cells.** Natarajan, Dipa; Boulter, Catherine A. (Dep. Genetics, Univ. Cambridge, Cambridge, UK CB2 3EH). *Nucleic Acids Res.* 1995, 23(19), 4003–4 (Eng). The authors constructed a gene trap vector, pβgyg, which is based on pSAβgeo which carries a βgeo fusion gene downstream of the splice acceptor site from adenovirus major late transcript. Essentially, the neo gene and polyA site from pSAβgeo has been replaced with a hygromycin B phosphotransferase (hyg) gene and phosphoglycerate kinase polyA site from pKJ23 such that the hyg gene is in frame with the lacZ gene to generate the fusion gene βgyg. The fusion gene is functional in mammalian cells, and the fusion protein retains biol. activity. This is the first report of hygromycin as a C-terminal fusion protein with β-galactosidase.

124: 1754q **Construction of specific cosmids from YACs by homologous recombination in yeast.** Herzing, Laura B. K.; Ashworth, Alan (CRC Cent. Cell Mol. Biol., Chester Beatty Lab., Inst. Cancer Res., London, UK SW3 6JB). *Nucleic Acids Res.* 1995, 23(19), 4005–6 (Eng). A method using homologous recombination in yeast was devised to engineer cosmids contg. precisely the sequence of interest, along with specific marker, reporter, or selection genes as desired. The strategy is to flank the sequence of interest by phage lambda cos sites. This configuaration will be recognized by lambda packaging exts. in the same way as would an integrted lambda genome; the sequence between the 2 cos sites is excised by cleavage within the cos sites, and packaged into lambda particles. The cosmid, circularized upon transduction into Escherichia coli can then be rescued. The resultant cosmid constructions are potentially suitable for transfection and transgenic expts. The only requirements for this procedure are yeast carrying a YAC contg. the gene of interest, and small amts. of cloned 5' and 3' sequence flanking the sequence to be cloned.

1995, 16(8), 1437–40 (Eng). The apolipoprotein B (apoB) variable no. of tandem repeat (VNTR) alleles contg. larger repeat units is a risk factor for coronary heart disease. Capillary electrophoresis (CE) in entangled polymer soln. was applied to the anal. of polymerase chain reaction (PCR) amplified apoB VNTR locus for DNA diagnosis of heart disease. The CE sepn. gives an excellent resoln. of two alleles differing by one or two 16 bp repeat units in the DNA size range up to 600 bp with high speed. The apoB alleles differing in length by 2 or 4 repeat units are readily distinguishable by CE in the DNA size range from 600 to 1000 bp. The plate no. achieved was 1 million plates per m. cE combining with PCR provides an excellent technique for accurate detn. of the no. of repeat units of apoB VNTR alleles and differentiation of heterozygous from homozygous individuals. Using the CE technique, the apoB VNTR loci from some individuals in genotyping were examd. towards precise DNA diagnosis for coronary heart disease.

123: 219491c **Enhanced transduction efficiency of retroviral vectors coprecipitated with calcium phosphate.** Morling, F. J.; Russell, S. J. (Cambridge Centre Protein Engineering, MRC Centre, Cambridge, UK CB2 2QH). *Gene Ther.* 1995, 2(7), 504–8 (Eng). Retroviral vectors are being used increasingly in clin. gene therapy protocols but low transduction frequencies are presenting a significant obstacle to progress. In this paper the authors report a simple method to enhance the efficiency of ex vivo retroviral gene transfer. Calcium chloride is added to the vector stock and calcium phosphate ppts. out of soln. in complex with the retroviral vectors. When such copptd. vectors were used for gene transfer, the vector titers were increased at least five–fold and as much as 50–fold compared with the titers obtained in std. polybrene–enhanced infection protocols. Titer enhancement was not dependent on the starting concn. of vector, was equally effective for ecotropic and amphotropic vectors on a variety of mouse and human cells, and was not assocd. with any alteration in vector host range properties. The method may be of value to conc. retroviral vectors and to enhance the efficiency of gene transfer in selected human gene therapy protocols.

123: 219492d **Efficient recovery of infectious vesicular stomatitis virus entirely from cDNA clones.** Whelan, Sean P. J.; Ball, L. Andrew; Barr, John N.; Wertz, Gail T. W. (Dep. Microbiology, Univ. Alabama Birmingham, Birmingham, AL 35294 USA). *Proc. Natl. Acad. Sci. U. S. A.* 1995, 92(18), 8388–92 (Eng). Infectious vesicular stomatitis virus (VSV), the prototypic nonsegmented neg.–strand RNA virus, was recovered from a full–length cDNA clone of the viral genome. Bacteriophage T7 RNA polymerase, expressed from a recombinant vaccinia virus, was used to drive the synthesis of a genome–length pos.–sense transcript of VSV from a cDNA clone in baby hamster kidney cells that were simultaneously expressing the VSV nucleocapsid protein, phosphoprotein, and polymerase from sep. plasmids. Up to 10^5 infectious virus particles were obtained from transfection of 10^6 cells, as detd. by plaque assays. This virus was amplified on passage, neutralized by VSV–specific antiserum, and shown to possess specific nucleotide sequence markers characteristic of the cDNA. This achievement renders the biol. of VSV fully accessible to genetic manipulation of the viral genome. In contrast to the success with pos.–sense RNA, attempts to recover infectious virus from neg.–sense T7 transcripts were uniformly unsuccessful because T7 RNA polymerase terminated transcription at or near the VSV intergenic junctions.

123: 219493e **The limits in electron microscopy of macromolecular interactions. The use of new labels based on lanthanide cryptates. An interdisciplinary approach.** Delain, Etienne; Barbin–Arbogast, Agnes; Bourgeois, Claire A.; Mathis, Gerard; Mory, Claudie; Favard, Cyril; Vigny, Paul; Niveleau, Alain (Lab. microscopie cellulaire et moleculaire, Inst. Gustave Roussy, F94805 Villejuif, Fr.). *J. Trace Microprobe Tech.* 1995, 13(3), 371–81 (Eng). Mol. cages made of europium cryptates bound to anti–5–mC antibodies were tested to localize this modified DNA base in metaphase human chromosomes. Eu, trapped in cryptates, can be detected using its fluorescence and electron energy loss properties. The conditions for optimal detection were analyzed using UV light microscopy, microspectrofluorimetry, and two electron microscopes equipped with spectrometers. The feasibility of using such cryptates was tested by electron microscopy; their use as fluorescent labels are still under investigation. The possibilities of improving this new labeling system are discussed.

123: 219494f **Selectable insertion and deletion mutagenesis of the human cytomegalovirus genome using the Escherichia coli guanosine phosphoribosyl transferase (gpt) gene.** Greaves, Richard F.; Brown, Janice M.; Vieira, Jeffrey; Mocarski, Edward S. (Dep. Microbiology, Stanford Univ. School Medicine, Stanford, CA 94305–5402 USA). *J. Gen. Virol.* 1995, 76(9), 2151–60 (Eng). We describe the mutagenesis of the IRS1–US5 region of the human cytomegalovirus genome, demonstrating the potential of the E. coli guanosine phosphoribosyl transferase (gpt) gene as a selectable marker for insertion and deletion mutagenesis of high passage (AD169, Towne) as well as low passage (Toledo) strains of virus. Despite evidence suggesting that the US3 gene product may play a regulatory role, disruption of this gene with a gpt insert had no effect on growth of any of these strains of virus in resting or dividing human fibroblasts, or in human thymus plus liver implants in SCID–humice. Transcripts of the gpt gene, under control of the herpes simplex virus thymidine kinase promoter adjacent to the US3 enhancer in the viral genome, accumulated with delayed early (β) kinetics. Mutants with deletions in the IRS1 and US3–US5 regions were isolated by back–selection against gpt with the drug 6–thioguanine by growing virus in human Lesch–Nyhan (hypoxanthine–guanine phosphoribosyl transferase deficient) skin fibroblasts immortalized with human papillomavirus oncogenes. Thus, we demonstrate a dependable method for insertion and deletion mutagenesis that can be applied to any region of the viral genome.

123: 219495g **Evaluation of prokaryotic diversity by restrictase digestion of 16S rDNA directly amplified from hypersaline environments.** Martinez–Murcia, A. J.; Acinas, S. G.; Rodriguez–Valera, F. (Departamento de Genetica y Microbiologia, Universidad de Alicante, Campus de San Juan, Apartado 374, Alicante, Spain E–03080). *FEMS Microbiol. Ecol.* 1995, 17(4), 247–55 (Eng). A novel mol. strategy to study microbiol. diversity is described. This method is based on the restriction digestion of a population of 16S rDNA sequences directly amplified from environmental samples. Digested fragments sepd. by polyacrylamide electrophoresis generate characteristic profile data for estn. of diversity and overall similarities between the organisms of different environments. The methodol. has been applied to a set of five ponds in a multi–pond solar saltern covering the salinity gradient from about twice that of seawater (6.4%) to NaCl pptn. (30.8%). Bacterial (eubacterial) diversity estd. from the complexity of the banding pattern obtained by restriction of the amplicons from the different ponds decreased with increasing salinity, while for Archaea (archaebacteria) the reverse was true; i.e., the higher the salinity the higher the no. of bands. The similarities in taxonomic compn. of the prokaryotic populations present in those ponds were evaluated from the no. of restriction bands shared by the different samples. The relationships found among the different environments were independent of the enzyme used for digestion and were consistent with previous descriptions obtained by the study of isolates from the different environments. The technique appears to be promising as a rapid method for microbial biodiversity fingerprinting. It is useful for comparisons of several environments and detection of major shifts in species compn. of the microbial population.

123: 219496h **SYBR Green I DNA staining increases the detection sensitivity of viruses by polymerase chain reaction.** Karlsen, Frank; Steen, Harald B.; Nesland, Jahn M. (Department of Pathology, The Norwegian Cancer Society, Oslo, Norway). *J. Virol. Methods* 1995, 55(1), 153–6 (Eng). The nucleic acid dye, SYBR Green I (Mol. Probes, Eugene, OR) has been designed esp. for staining of DNA of less than 20 pg following agarose or polyacrylamide gel electrophoresis. The performance of this dye in comparison with ethidium bromide was measured using the detection of human papillomavirus 16 PCR products as a test. Briefly, SYBR Green I was much more sensitive than ethidium bromide and was less dependent on DNA strand length for staining.

123: 219497j **Method for constructing internal standards for use in competitive PCR.** Zarlenga, Dante S.; Canals, Ana; Gasbarre, Louis (U.S. Department Agriculture, Agricultural Research Service, Beltsville, MD USA). *BioTechniques* 1995, 19(3), 324–6 (Eng). A method for construction of internal competitor DNA mols. from previously cloned sequences for use as stds. in reverse transcription–polymerase chain reaction is described. Construction of the competitor DNAs requires a single PCR amplification using a previously cloned sequence and two primers, sepd. by a predefined distance, that amplify in opposite directions, and, in so dioing, encompass the entire vector during amplification. An advantage of this method is its speed; competitor mols. can be constructed in a single day. Addnl., competitor mols. can be differentiated from native cDNAs by simple restriction enzyme digestion at the restriction site incorporated into the competitor DNA.

123: 219498k **Background reduction in Northern analysis by preabsorption of digoxigenin–labeled riboprobes.** Sprenger, Hans; Konrad, Lutz; Rischkowsky, Elfi; Gemsa, Diethard (Philipps–University Marburg, Marburg, Germany). *BioTechniques* 1995, 19(3), 334, 336, 338, 340 (Eng). A method is presented for significantly reducing the background in non–radioactive Norhtern anal. by preabsorption of digoxigenin–labeled riboprobes to total RNA fixed on pos. charged nylon membranes. The method was successfully used to detect macrophage inflammatory protein MIP–1α and RANTES protein mRNA with minimal, non–specific background hybridization. This background redn. enables extension of exposure times and subsequent increases in the sensitivity of mRNA detection.

123: 219499m **Dual temperature in situ hybridization.** Weier, Heinz–Ulrich G.; Greulich, Karin M.; Young, David M. (Lawrence Berkeley Laboratory, University California, Berkeley, CA USA). *BioTechniques* 1995, 19(3), 364–6 (Eng). A dual temp. fluorescence in situ hybridization method for easy, sensitive detection of DNA is described. The advantages of this method include: washing steps can be omitted, hybridization signals can be obsd. as early as one day after DNA probe application, and hybridization signals are very stable.

123: 219500e **Improvement of fluorescence in situ hybridization (RNA–FISH) on human paraffin sections by propidium iodide counterstaining.** Wulf, Martin; Bosse, Alexander; Voss, Bruno; Mueller, Klaus–Michael (Institute Pathology, University Clinic, Bergmannsheil, Germany). *BioTechniques* 1995, 19(3), 368, 370, 372 (Eng). A method using fluorescence in situ hybridization in combination with propidium iodide counterstaining is presented for demonstration of mRNA expression in paraffin–embedded tissues. This method was used to demonstrate transforming growth factor β mRNA expression in different paraffin–embedded bone tissues.

123: 219501f **Mini–preparation of total RNA for RT–PCR from cultured human cells.** Ogretmen, Besim; Safa, Ahmad R. (University Chicago, Chicago, IL USA). *BioTechniques* 1995, 19(3), 374–6 (Eng). A modification of the sodium dodecyl sulfate/phenol RNA extn. method has been developed to allow isolation of undegraded, DNA–free, total RNA from a low no. of cultured human

mRNA levels, a sensitive and quant. assay is required. A quick and easy method is described to quantify specific mRNA's by a combination of the polymerase chain reaction (PCR) and an electro-chemiluminescent (ECL) detection of the amplified products. Total cellular RNA is reverse transcribed and amplified with a biotinylated forward primer and a TBR [Tris(2,2'-bipyridine)ruthenium(II)] labeled reverse primer. The amplification product is captured on streptavidin-coated paramagnetic beads and quantified by ECL detection using the QPCR system 5000. The results can be converted to quant. values with an external std. curve. In the present study, cytokine mRNA expression in T lymphocytes was quantified. Cytokine mRNA was measured at the attomolar range in a dynamic range up to three orders of magnitude. The ECL detection is quant., rapid and accurate.

123: 219449v **Determination of human cytomegalovirus (HCMV) immediately early gene (IEG) and late gene (LG) fragments by polymerase chain reaction (PCR).** Chen, Ruizhen; Yang, Yingzhen; Jin, Peiying (Zhongshan Hosp., Shanghai Med. Univ., Shanghai, Peop. Rep. China 200032). *Zhonghua Yixue Jianyan Zazhi* 1995, 18(2), 95–8 (Ch). The IEG and LG fragments extd. from human embryonic fibroblast (HEF) cells infected with HCMV and clin. samples were detd. by PCR. The results showed that the pos. rates of IEG and LG were 8% and 33% in kidney transplantation patients and 20% and 50% in atherosclerosis patients, resp. Neither false pos. nor neg. results were found. Thus, the method might be widely used in clin. diagnosis as well as in basic research of HCMV infection.

123: 219450p **Development of a species-diagnostic polymerase chain reaction assay for the identification of Culex vectors of St. Louis encephalitis virus based on interspecies sequence variation in ribosomal DNA spacers.** Crabtree, M. B.; Savage, H. M.; Miller, B. R. (Arbovirus Diseases Branch, Div. Vector-Borne Infectious Diseases, National Center Infectious Diseases, Centers Disease Control, Prevention, Fort Collins, CO USA). *Am. J. Trop. Med. Hyg.* 1995, 53(1), 105–9 (Eng). Culex pipiens complex mosquitoes (Cx. p. pipiens and Cx. p. quinquefasciatus) are among the principal vectors of St. Louis encephalitis (SLE) virus in the eastern United States; Cx. restuans and Cx. salinarius play secondary roles in the transmission and maintenance of the virus cycle. Accurate identification of these three species in field collections is required for epidemiol. studies of SLE virus transmission. We have developed a polymerase chain reaction (PCR) assay for this purpose. Species-specific PCR primers were designed based on interspecies nucleic acid sequence variation in the first and second internal transcribed spacers (ITS1 and ITS2) of the nuclear ribosomal DNA gene array; however, insufficient variation was detected to differentiate between subspecies of the Cx. pipiens complex. The primers were used together in a single amplification reaction to correctly identify specimens to species using genomic DNA extd. from whole individual mosquitoes, DNA from triturated mosquito pools, or crude DNA from mosquito heads or legs.

123: 219451q **Nonradioactive detection of hypervariable simple sequence repeats in short polyacrylamide gels.** Morin, Phillip A.; Smith, David Glenn (Univ. California, Davis, CA USA). *BioTechniques* 1995, 19(2), 223–26, 227 (Eng). A method for resolving and visualizing genotypes for simple sequence repeat loci on short (20 cm) polyacrylamide gels is described. This method makes use of a modified vertical electrophoresis cell to allow rapid electrophoresis without variation in migration rates due to uneven gel heating. Gels are stained with SYBR™ Green to visualize and photograph bands on an UV transilluminator, thereby eliminating for need for traditional radioisotope labeling of PCR products for autoradiog.

123: 219452r **Mutagenesis using trinucleotide β-cyanoethyl-phosphoramidites.** Lyttle, Matthew H.; Napolitano, W.; Calio, Brenda L.; Kauvar, Lawrence M. (Terrapin Technologies, San Francisco, CA USA). *BioTechniques* 1995, 19(2), 274–8, 280–1 (Eng). There is no easy way to selectively introduce mixts. of codon triplets into mutagenesis libraries. Solid-phase-supported DNA synthesis using successive coupling of mixts. of mononucleotides can be made to supply 32 codons, which gives redundancies in coding for 20 natural amino acids, as well as an often unwanted stop codon. Resin-splitting methods have been described, but the representation of all permutations is limited by mech. factors for a large library, and the method is exptly. cumbersome. To demonstrate a third, improved method, the 3'-cyanoethyl phosphoramidite codon triplets dATA, dCTT, dATC, dATG and dAGC were made by soln.-phase methods, with protecting groups fully compatible with modern automated phosphoramidite DNA synthesis chem. The reagents were then used to synthesize a 54-mer DNA fragment, wherein 15 internal base pairs were randomized by coupling a mixt. of the five codons five times. The fragment was amplified as a cDNA pool, which was sub-cloned into a phagemid vector, and 16 randomly selected recombinants from this mini-library were sequenced. These clones showed random incorporation of the proper transcribed codon sequences at the correct location. Other functional tests involving the trinucleotide phosphoramidites showed modest (ca. 70%) coupling efficiencies and structural integrity of the DNA produced.

123: 219453s **Rapid HCV RNA detection by PCR followed by a new non-radioactive liquid hybridization assay and comparison with RIBA.** Schacker, Ulrike; Bermayer, Hans-Peter; Boehler, Valerie; Ionescu, Doina; Zapata, Manuel; Grauer, Hasan; Rai, Kamal (Medical Diagnostic Laboratory, Baden-Baden, Germany). *J. Med. Virol.* 1995, 46(4), 304–9 (Eng). A one-stage polymerase chain reaction (PCR) followed by an automated, liq. hybridization assay was used to examine anti-HCV-pos. patients. The presence of HCV-RNA in 251 randomly selected enzyme immunoassay (EIA) pos. clin. specimens was compared to their RIBA pattern. As assocn. of a RIBA pattern with presence or absence of HCV-RNA was not detected. One hundred of these samples were also evaluated after dividing them into normal and elevated serum alanin aminotransferase (ALT) levels. PCR results were obtained on the basis of amplification products from two different gene regions (5'-NC region and NS 3). To prove the specificity of the PCR products, a com. available digoxigenin-based liq. hybridization assay was evaluated. The sensitivity was comparable to the results obtained after nested PCR. Based on the results of the study, the two-stage PCR can be changed in favor of the easier one-step PCR which offers the advantage of fewer contamination problems.

123: 219454t **Cre-mediated site-specific translocation between nonhomologous mouse chromosomes.** van Deursen, J.; Fornerod, M.; van Rees, B.; Grosveld, G. (Dep. Genet., St. Jude Children's Res. Hsop., Memphis, TN 38105 USA). *Proc. Natl. Acad. Sci. U. S. A.* 1995, 92(16), 7376–80 (Eng). Chromosome rearrangements, such as large deletions, inversions, or translocations, mediate migration of large DNA segments within or between chromosomes, which can have major effects on cellular genetic control. A method for chromosome manipulation would be very useful for studying the consequences of large-scale DNA rearrangements in mammalian cells or animals. With the use of the Cre-loxP recombination system of bacteriophage P1, we induced a site-specific translocation between the Dek gene on chromosome 13 and the Can gene on chromosome 2 in mouse embryonic stem cells. The estd. frequency of Cre-mediated translocation between the nonhomologous mouse chromosomes in approx. 1 in 1200–2400 embryonic stem cells expressing Cre recombinase. These results demonstrate the feasibility of site-specific recombination systems for chromosome manipulation in mammalian cells in vivo, breaking ground for chromosome engineering.

123: 219455u **Coupling- and repulsion-phase RAPDs for marker-assisted selection of PI 181996 rust resistance in common bean.** Johnson, E.; Miklas, P. N.; Stavely, J. R.; Martinez-Cruzado, J. C. (Tropical Agric. Res. Stn., ARS, Mayaguez, P. R. 00681). *Theor. Appl. Genet.* 1995, 90(5), 659–64 (Eng). The Guatemalan black bean (Phaseolus vulgaris L.) plant introduction (PI) 181996 is resistant to all known US races of the bean rust fungus Uromyces appendiculatus appendiculatus. Two random amplified polymorphic DNA (RAPD) markers, $OAC20_{490}$ tightly linked (no recombinants) in coupling phase and $OAE19_{880}$ linked in repulsion phase (at 6.2±2.8 cM) to PI 181996 rust resistance, are reported. These RAPDs, generated by single decamer primers in the polymerase chain reaction, were identified in near-isogenic bulks of non-segregating resistant and susceptible BC_4F_2 (NX-040*4/PI 181996) lines. Linkage of the RAPD markers was confirmed by screening 19 BC_4F_2 and 57 BC_4F_3 individuals segregating for PI 181996 resistance. Utility of the RAPDs $OAC20_{490}$ and $OAE19_{880}$ was investigated in a diverse group of common bean cultivars and lines. All cultivars into which the PI 181996 resistance was introgressed had the RAPD $OAC20_{490}$. A RAPD similar in size to $OAC20_{490}$, obsd. in some susceptible common bean lines, was confirmed by Southern blotting to be homologous to the RAPD $OAC20_{490}$. Use of the RAPDs $OAC20_{490}$ and $OAE19_{880}$ in marker-assisted selection (MAS) is proposed. The coupling-phase RAPD is most useful for MAS of resistant BC_4F_3 individuals during traditional backcross breeding. The repulsion-phase RAPD has greatest utility in MAS of homozygous-resistant individuals in F_2 or later-segregating generations.

123: 219456v **Assessment of stress gene mRNAs (HSP-27, 60 and 70) in obstructed rabbit urinary bladder using a semi-quantitative RT-PCR method.** Zhao, Yang; Wein, Alan J.; Levin, Robert M. (Div. Urology, Univ. Pennsylvania, Philadelphia, PA USA). *Mol. Cell. Biochem.* 1995, 148(1), 1–7 (Eng). Stress proteins (HSPs) participate in the cellular response to various stresses including hyperthermia, hypoxia and injury. A previous work using northern blot anal. demonstrated increased expression of stress protein 70 (HSP-70) in rabbit bladder tissue subjected to partial outlet obstruction. In order to det. if the increased expression was specific for HSP-70 or, alternatively, indicated a generalized stress protein response, a modified quant. RT-PCR technique was used to quantitate HSP mRNAs (HSP-27, 60, and 70) in normal and obstructed rabbit urinary bladder tissues. The results show the following: 1) The modified semi-quant. RT-PCR is a sensitive and reproducible technique for detecting mRNA in bladder tissue. 2) Constitutive levels of HSP-27, HSP-60, and HSP-70 mRNAs were detected in control bladder tissues; the relative signal intensity was largest for HSP-70 and lowest for HSP-27.3) A transient increase in HSP mRNAs was obsd. after obstruction; the mRNA of HSP-27, 60 and 70 increased 4.3-, 5.6-, and 2.4-fold, resp., at 24 h following obstruction, then gradually returned to control levels by the end of one week post-obstruction and remained stable up to 14 days post-obstruction. These data indicate that the modified quant. RT-PCR is a useful technique for detecting mRNA in bladder tissue; the stress response which occurs in rabbit urinary bladder tissue following partial outlet obstruction is a general phenomenon.

123: 219457w **A rapid and highly efficient method for PCR-based site-directed mutagenesis using only one new primer.** Boles, Eckhard; Miosga, Thomas (Institut Mikrobiologie, Technische Hochschule Darmstadt, D-64287, Darmstadt, Germany). *Curr. Genet.* 1995, 28(2), 197–8 (Eng). The authors present a rapid, cheap and highly efficient method for site-directed mutagenesis using the polymerase chain reaction (PCR). This method is applicable to every DNA fragment which has to be cloned into the multiple cloning site of any vector, or vector pair, in two different orientations. It requires only two primers, one new and specific

Zhendong; Wei, Zhiming; Xu, Zhihong (Shanghai Inst. Plant Physiol., Acad. Sin., Shanghai, Peop. Rep. China 200032). *Shiyan Shengwu Xuebao* 1994, 27(3), 341–51 (Ch). Foreign genes were introduced into protoplasts of Brassica napus L. by means of PEG treatment. Gene transfer efficiency was found to be influenced by two-valence cations and their concns. in transformation mixt., by addn. of carrier DNA, and by pH of PEG soln. With hygromycin or kanamycin resistance as selection markers, resistant calli were successfully recovered. The relative transformation frequencies for hygromycin resistance was 1.3%, being distinctly higher than 0.2% for kanamycin resistance. Thereafter, resistant calli were transferred onto differentiation medium for shoot induction. After regenerated shoots were rooted on rooting medium, they were transplanted into pots. Most of them grew well, Enzyme assay and Southern blotting anal. showed that foreign genes has been integrated into plant genomes. Lower frequency of shoot differentiation from resistant calli was the main problem in the gene transfer system reported here, some reasons for which were suggested.

123: 2063e **Detection of ovine progressive pneumonia proviral cDNAs with polymerase chain reaction.** Ding, Enyu; Xiang, Wenhua (School Life Sciences, Fudan Univ., Shanghai, Peop. Rep. China 200433). *Bingdu Xuebao* 1994, 10(2), 187–9 (Ch). Using the PCR method, the proviral cDNAs of sheep fetal lung cells infected by ovine progressive pneumonia virus (OPPV) and the peripheral blood monocytes in sheep infected by OPPV were detected. The initial time of OPP proviral cDNA integrated into sheep fetal lung cells was 24 h postinoculation and the initial time of OPP proviral cDNA integrated into the peripheral blood monocytes in sheep was 9 days postinoculation. The PCR method is one of the best methods for the rapid and specific diagnosis of OPP and other lentivirus diseases.

123: 2064f **Hepatitis C virus RNA detection and HCV genotype in patients with chronic non-A, non-B hepatitis in Jakarta.** Widjaja, Suwandhi; Li, Sheng; Ali, Sugianto; Simon, Sumanto; Sulaiman, Ali; Lesmana, L. A.; Yap, Sing Hiem (Hepatitis Research Unit, Atmajaya Medical Faculty, University of Atmojaya, Jakarta, Indonesia). *J. Virol. Methods* 1995, 51(2,3), 169–76 (Eng). Antibody response in HCV infection may be variable and the variability of the serol. response could be due to the differences in HCV strains. Since the distribution of hepatitis C virus genotype has been found to be geog. dependent, it is important to det. the distribution of HCV genotype in various countries with high prevalence of chronic non-A, non-B hepatitis. In this study, serum HCV RNA was examd. in 53 patients suspected of chronic non-A, non-B hepatitis with an anti-HCV test as detd. by currently available assay. HCV viremia was detected in 48 patients (90.6%). These patients had elevated serum ALT level at the time of HCV RNA detn. Using specific genotype probes, all isolates were classified into three different genotypes. Double and triple infections were also noted. HCV genotype 1b is the predominant genotype found in chronic hepatitis C patients in Jakarta.

123: 2065g **Apolipoprotein E genotyping.** Prins, J.; Tilanus, M. G. J.; van Rijn, H. J. M. (Laboratorium voor Klinische Chemie, Academisch Ziekenhuis, 3508 GA Utrecht, Neth.). *Tijdschr. Ned. Ver. Klin. Chem.* 1994, 19(6), 308–12 (Eng). Apolipoprotein E (apoE) pheno- or genotyping can be used to discriminate between the common apoE isotypes, namely apoE2, apoE3 and apoE4. ApoE2, a dysfunctional mutant of apoE3, is assocd. with familial dysbetalipoproteinemia, a disorder assocd. with premature atherosclerosis caused by the accumulation of chylomicron- and VLDL-remnants in plasma. For genotyping, the apoE fragment spanning the polymorphic sites (codons 112 and 158) is amplified by PCR. This article deals with the possibility of apoE genotyping by restriction isotyping or allele-specific probes. For restriction isotyping an improved primer set is used in the PCR, subsequently the PCR-product is digested by CfoI and subjected to electrophoresis on polyacrylamide gel, leading to a unique combination of CfoI fragment sizes for each genotype. For genotyping with allele-specific probes a com. available kit is used in which the PCR-product, dependent on its genotype, will or will not hybridize with strips annealed with allele-specific probes. Both methods unambiguously allowed apoE genotyping. On financial grounds the method based on apoE restriction isotyping is chosen in our lab. for performing apoE genotyping.

123: 2066h **Use of URA3 as a reporter of gene expression of C. albicans.** Myers, Kristi K.; Sypherd, Paul S.; Fonzi, William A. (Genprobe, San Diego, CA 92121 USA). *Curr. Genet.* 1995, 27(3), 243–8 (Eng). The C. albicans URA3 gene was tested as a reporter of gene expression. An integrating vector was constructed which contained ADE2 as a selectable marker together with a truncated form of URA3 lacking the first three codons. A DNA fragment contg. the promoter and the first 90 codons of the C. albicans CEF3 gene was inserted into the unique XhoI site 5' to URA3 in order to provide an in-frame translational fusion. The functionality of the fusion gene was tested following integration of a single copy of the plasmid into the ADE2 locus. The fusion gene was shown to complement a ura3 deletion mutation and to produce orotidine 5'-monophosphate decarboxylase activity (OMP), which is encoded by URA3. Expression of the fusion gene was appropriately regulated by the growth rate and utilized the same transcriptional start sites as the native CEF3 gene. The results demonstrate that URA3 provides a sensitive and versatile reporter gene for use in C. albicans.

123: 2067j **Transposon mutagenesis of coryneform bacteria.** Vertes, Alain A.; Asai, Yoko; Inui, Masayuki; Kobayashi, Miki; Kurusu, Yasurou; Yukawa, Hideaki (Tsukuba Research Center, Mitsubishi Petrochemical Co., Ltd., Inashiki, Ibaraki, Japan 300-03). *Mol. Gen. Genet.* 1994, 245(4), 397–405 (Eng). The Corynebacterium glutamicum insertion sequence IS31831 was used to construct two artificial transposons: Tn31831 and minTn31831. The transposition vectors were based on a gram-neg. replication origin and do not replicate in coryneform bacteria. Strain Brevibacterium flavum MJ233C was mutagenized by minTn31831 at an efficiency of 4.3×10^4 mutants per μg DNA. Transposon insertions occurred at different locations on the chromosome and produced a variety of mutants. Auxotrophs could be recovered at a frequency of approx. 0.2%. Transposition of IS31831 derivs. led not only to simple insertion, but also to cointegrate formation (5%). No multiple insertions were obsd. Chromosomal loci of B. flavum corresponding to auxotrophic and pigmentation mutants could be rescued in Escherichia coli, demonstrating that these transposable elements are useful genetic tools for studying the biol. of coryneform bacteria.

123: 2068k **Development of PCR assays to detect genetic variation amongst equine herpesvirus-1 isolates as an aid to epidemiological investigation.** McCann, S. H. E.; Mumford, J. A.; Binns, M. M. (Department of Infectious Diseases, Animal Health Trust, Lanwades Park, Kennett, Newmarket, Suffolk, UK CB8 7PN). *J. Virol. Methods* 1995, 52(1,2), 183–94 (Eng). A search for variable restriction sites has been carried out for equine herpesvirus-1 (EHV-1) in an attempt to develop markers which can be used to group epidemiol. related viruses into groups, and to learn more about the dynamics of EHV-1 disease. Crude viral DNA exts. of EHV-1, prepd. by Hirt extn., were digested with AluI, HaeIII, or RsaI, and Southern blotted following electrophoresis. DNA fingerprints, produced by probing the Southern blots with the EHV-1 EcoR1-I fragment, sepd. 56 isolates into 16 groups. The variable sites within the EcoR1-I fragment were mapped approx. using fragments from within EcoR1-I, and the precise location of the variable sites detd. from the DNA sequence of this fragment. Oligonucleotide primers flanking the variable sites were synthesized, and used in PCR assays to detect variable fragments. The AluI variable fragment was the result of the the presence or absence of a single AluI site. In contrast, the variable bands seen with HaeIII and RsaI, resulted from variation in the copy no. of two tandemly repeated sequences, one of which had not previously been recognized. In addn., HaeIII digests of EHV-1 isolates probed with the glycoprotein B (gB) gene of EHV-1 also sepd. isolates into two groups. The variable HaeIII site was mapped towards the 5'-end of the gB gene and a PCR assay established. The distribution of the variable AluI site within the EcoRI-I fragment and the HaeIII site within the gB gene were estd. on a large no. of clin. isolates using PCR on unpurified viral tissue culture medium. Both sites had a good distribution and together with addnl. variable sites should provide the basis for the rapid DNA fingerprinting of EHV-1 isolates.

123: 2069m **Background-minimized cassette mutagenesis by PCR using cassette-specific selection markers: a useful general approach for studying structure-function relationships of multisubstrate enzymes.** Majumder, Kumud; Fattah, Farkad A.; Selvapandiyan, Angamuthu; Bhatnagar, Raj K. (Plant Mol. Biol. Lab., Intl. Cent. Gen. Eng. Biotechnol., New Delhi, 110 067 India). *PCR Methods Appl.* 1995, 4(4), 212–18 (Eng). An efficient protocol, termed background-minimized cassette mutagenesis (BMCM) by PCR, has been developed for multiple mutagenesis of DNA. This method uses suitable extension primers for incorporating various mutation(s) and is not limited by either the nature of the mutation or the size and spatial location of mutational loci. Minimization of the wild-type background clone and mutant selection at very high frequency were easily achieved through a 2-step process. First, a deletion of a unique restriction site within the cassette was introduced through addnl. silent mutation(s). Then, the recombinant clones were digested with the corresponding enzyme followed by transformation when selective linearization of wild-type clone led to its near total removal leaving the mutant clones as the only practicable transformants. Because it is generally possible to design several such cassette-specific unique background minimization markers for any gene, for multiple mutagenesis involving distally located portions of the gene the present protocol is superior to other currently available methods. The efficiency of BMCM-PCR has been demonstrated here by using the multisubstrate enzyme 5-enolpyruvyl-shikimate-3-phosphate synthase (EPSPs) of Bacillus subtilis as a model system. Three different sets of cassettes of varying sizes were generated to encompass the three putative active/binding regions in the beginning, middle, and the end of the gene encoding EPSPs. Very high efficiency of mutation incorporation and selection were obtained in all cases. Furthermore, by taking advantage of the unique cassette-specific background elimination markers, it was possible to generate a nested set of double and/or triple mutants. The mutant enzymes were overexpressed in Escherichia coli and purified to near homogeneity. Comparison of the kinetic data of these mutants with the wild-type enzyme provided important insight into the mechanism of the binding of EPSPs to its multiple substrates. Significantly, the present concept of background minimization can be easily extended to most of the other methods of site-directed mutagenesis, thereby improving the performances of these methods.

123: 2070e **Quantitative detection of reverse transcriptase-PCR products by means of a novel and sensitive DNA stain.** Schneeberger, Christian; Speiser, Paul; Kury, Fritz; Zeillinger, Robert (Dep. Obstetrics Gynecol., Univ. Vienna, Vienna, Austria). *PCR Methods Appl.* 1995, 4(4), 234–8 (Eng). A plasmid was constructed for the in vitro synthesis of a competitor RNA for use as an internal exogenous control during reverse transcriptase-PCR (RT-PCR) detection of epidermal growth factor receptor (EGFR) expression. The competitor RNA harbors a 32-base deletion

compared with wild-type EGFR mRNA and generates a PCR product that is easily distinguished from the wild-type PCR product by agarose gel electrophoresis. The problem of heteroduplex formation was encountered during later stages of PCR, which could be solved by decreasing the PCR cycle no. This was accompanied by a significant loss of sensitivity. Sensitivity could be restored by using a novel and extremely sensitive DNA stain (SYBR Green I) instead of ethidium bromide.

123: 2071f **Identification of the species origin of highly processed meat products by mitochondrial DNA sequences.** Unseld, Michael; Beyermann, Birgit; Brandt, Petra; Hiesel, Rudolf (Inst. Genbiol. Forschung, 14195 Berlin, Germany). *PCR Methods Appl.* 1995, 4(4), 241 (Eng). Mitochondrial cytochrome b sequences were used for identification of cooked and canned tuna fish species in com. prepns. Five different tuna speices were identified in a total of 30 com. distributed cans. The mol. methods used were PCR in conjunction with cloning and subsequent sequence anal. The specificity of the PCR primers used for the amplification of degraded tuna DNA is not restricted to fish sequences, but can also amplify human DNA isolated from hair roots and pork DNA isolated from cooked susages. Thus, is now feasible to det. the fish meat sources of cans processed on mother ships and to clarify problems regarding quotas, protected species, customs declarations, and import/export restrictions.

123: 2072g **Detection of prostatic cells in peripheral blood: correlation with serum concentrations of prostate-specific antigen.** Jaakkola, Susanna; Vornanen, Timo; Leinonen, Jari; Rannikko, Sakari; Stenman, Ulf-Hakan (Dep. Clinical Chem. Obstetrics Gynecol., Helsinki Univ. Central Hosp., SF-00290 Helsinki, Finland). *Clin. Chem. (Washington, D. C.)* 1995, 41(2), 182-6 (Eng). The expression of prostate-specific antigen (PSA) mRNA was studied by reverse transcriptase-polymerase chain reaction in peripheral blood of 25 patients with cancer of the prostate (CAP), 4 with benign prostatic hyperplasia (BPH), 2 with renal stones, 3 with other types of cancer, and 6 healthy male and 3 female controls. Expression of mRNA specific for a certain tissue in peripheral blood is thought to indicate the presence of circulating cancer cells and metastatic spread of a tumor originating from this tissue. PSA mRNA was detected in 9 of 18 CAP patients with metastatic disease but in none of 7 patients without metastases. Neg. results in patients with metastatic disease were assocd. with successful endocrine therapy and low concns. of serum PSA, and the correlation between serum concns. of PSA and the presence of PSA mRNA in peripheral blood was statistically significant. PSA mRNA was not found in patients with BPH, other types of cancer, or in healthy controls. Thus, the occurrence of PSA mRNA in peripheral blood is assocd. with metastatic CAP.

123: 2073h **Improved PCR amplification/HhaI restriction for unambiguous determination of apolipoprotein E alleles.** Appel, Elena; Eisenberg, Shlomo; Roitelman, Joseph (Inst. Lipid Atherosclerosis Res., Sheba Med. Cent., 52621 Tel Hashomer, Israel). *Clin. Chem. (Washington, D. C.)* 1995, 41(2), 187-90 (Eng). A modification is presented for the polymerase chain reaction amplification/HhaI restriction isotyping method for human apolipoprotein (apo) E. This method includes a mutagenic forward primer and 5'-end labeling of both primers. These modifications of the original method described by J. E. Hixon and D. T. Vernier (1990) allow sensitive and unambiguous detn. of apoE genotypes.

123: 2074j **A non-radioactive single-strand conformation polymorphisms of asymmetric PCR and its application.** Chen, Jun; Wang, Huimin; Li, Manzhi; Wu, Yintang (Cancer Inst., Sun Yatsen Univ. Med. Sci., Canton, Peop. Rep. China 510060). *Shengwu Huaxue Yu Shengwu Wuli Jinzhan* 1994, 21(6), 550-3 (Ch). PCR-single strand conformation polymorphisms is a powerful method for screening mutations and widely used in studying mutations of oncogene and tumor suppressor gene. The ordinary PCR-SSCP needs the use of radioactivity and sequencing app., thus compromises its application. Here, a non-radioactive asym. PCR-SSCP was established. Single-stranded DNA was generated by asym. PCR, sepd. by mini PAGE and silver staining. Exons 5, 6, 7, 8 of p53 gene in four cell lines of nasopharyngeal carcinoma-CNE1, CNE2, HK1 and SUNE1 were investigated. The method was successful in screening mutations.

123: 2075k **PCR detection of Mycoplasma contamination in cell culture.** Wang, Zhengsen; Wu, Jianxin; Zhao, Xiaoyuan; Sun, Baoling; Guo, Zhanggai; Li, Min (Dep. Biochem. Immunol., Capital Inst. Pediatr., Beijing, Peop. Rep. China 100020). *Shengwu Huaxue Yu Shengwu Wuli Jinzhan* 1994, 21(6), 553-6 (Ch). Mycoplasma contaminatin of cell culture is a serious problem in biomedical research. Three common PCR primers (F1, F2 and R1) were designed to amplify the spacer region between 16s and 23s DNA in rRNA operons of 6 species of mycoplasmas (M. arginini, M. orale, M. hominis, M. hyorhinis, M. fementans and A. laidlawii). When the DNA of 6 species was used as the template, primers F1 and R1 produced fragments of 340 to 468 bp, and primers F2 and R1 produced fragments of 145 to 211 bp. No discrete band was obsd. in electrophoretic gels when Hela cell or E. coli DNA was served as the template with the use of primers F1 and R1. As little as 8.5 fg DNA of M. arginini, approx. 13 organisms could be detected. This suggests that mycoplasma contaminatin to cell cultures can be detected by PCR.

123: 2076m **Rapid production of digoxigenin labeled DNA probes by hot start PCR.** Li, Lijia; Zhang, Xiyuan; Jiang, Haibo (Life Sci. Coll., Wuhan Univ., Wuhan, Peop. Rep. China 430072). *Shengwu Huaxue Yu Shengwu Wuli Jinzhan* 1994, 21(6), 557-8 (Ch). A method for generating a nonradioactive digoxigenin (Dig) labeled probes is described. It was achieved by substituting the dTTP with Dig-11-dUTP and utilizing human genome DNA as template during the Hot Start PCR.

123: 2077n **A chromosome integration system for stable gene transfer into Thermus flavus.** Weber, J. Mark; Johnson, Scot P.; Vonstein, Veronika; Casadaban, Malcolm J.; Demirjian, David C. (ThermoGen, Inc., Chicago, IL 60612 USA). *Bio/Technology* 1995, 13(3), 271-5 (Eng). We have developed a chromosomal integration system for gene transfer into the extreme thermophile Thermus flavus. The system relies on integration at the site of leuB (3-isopropylmalate dehydrogenase) which was cloned from T. flavus. The leuB gene was insertionally inactivated in vitro with a thermostable kanamycin-resistance gene and transformed in single-copy into the chromosome of T. flavus on a plasmid vector. Gene replacement strains required leucine for growth, were stably kanamycin-resistant and could grow in the presence of kanamycin at temps. up to 55°C.

123: 2078p **Molecular identification of two distinct hemagglutinin types of measles virus by polymerase chain reaction and restriction fragment length polymorphism (PCR-RFLP).** Saito, Hiroyuki; Nakagomi, Osamu; Morita, Morihiro (Dep. Microbiology, Akita Prefectural Inst. Public Health, Akita, Japan 010). *Mol. Cell. Probes* 1995, 9(1), 1-8 (Eng). Contemporary isolates of measles virus, characterized by their inability to hemagglutinate, have been shown to possess a hemagglutinin type distinct from that of classical strains such as the Edmonston strain in that there is a new glycosylation site at amino acid residue 416. This change abolishes a Sau3AI site that is found in the corresponding position of the hemagglutination-pos. classical strains. This mol. information prompted us to develop a restriction fragment length polymorphism (RFLP) assay that is capable of distinguishing these two distinct hemagglutinin types. The assay consists of the amplification of a 349-bp segment of the hemagglutinin gene by reverse transcription followed by the polymerase chain reaction and Sau3AI digestion of this amplification product. The resulting two distinct RFLP patterns identified the hemagglutinin types with regard to the presence or absence of the potential new glycosylation site. This assay was applied to det. the relative frequencies over a 28-yr period of these two hemagglutinin types present in the archival acute serum specimens taken from patients with measles. This study revealed that strains carrying the classical hemagglutinin type predominated until the early 1980s when it became completely replaced with strains possessing the contemporary hemagglutinin type. Because of its direct applicability to the clin. specimens avoiding selection bias during cell-culture adaptation, this assay provides a valuable asset in both clin. lab. and epidemiol. settings.

123: 2079q **Detection of Legionellae with polymerase chain reaction.** Song, Yong; Kang, Xiaoming; Li, Zhenda (Department Respirology, PLA Nanjing General Hospital, Nanjing, Peop. Rep. China 210002). *Jiangsu Yiyao* 1994, 20(9), 466-8 (Ch). We have developed the method for detection of cultured Legionella, based upon the polymerase chain reaction (PCR). All 11 strains of Legionella (including all 8 serogroups of L. pneumophila) were detected by PCR amplification of a 104-bp DNA sequence that codes for a region of 5S rRNA with genus specific primers; and all 8 serogroups of L. pneumophila were detected by amplification of a 650 bp region of the coding region DNA sequences of the macrophage infectivity potentiator (mip) gene by species-specific primers. Bands of pos. amplified DNA were detected in 60 fg template DNA, our study suggested that this technique could be applied to clin. specimens for rapid identification and specific diagnosis of legionella disease, so that environmental monitoring and control of fulminant epidemic of legionellosis could be possible.

123: 2080h **Visual detection method for identifying recombinant bacterial colonies.** Austin, Richard C.; Singh, Davindra; Liaw, Patricia C. Y.; Craig, Hugh J. (Hamilton Civic Hosp. Res. Cent., McMaster Univ., Hamilton, ON Can.). *BioTechniques* 1995, 18(3), 380, 382, 383 (Eng). If a plasmid vector does not contain a convenient marker for selection, the ability to identify recombinants is lim- ited. We have now utilized a visual detection method for identifying recombinant bacterial colonies. This detection method is based solely on the morphol. of the transformed bacterial colony when grown on LB plates contg. ampicillin.

123: 2081j **Application of random amplified polymorphic DNA (RAPD) in thermal-sensitive nuclear male sterility in rice.** Zhang, Zhongting; Li, Songtao; Wang, Bin (Institute Genetics, Academia Sinica, Beijing, Peop. Rep. China 100101). *Yichuan Xuebao* 1994, 21(5), 373-8 (Ch). Random amplified polymorphic DNA (RAPD) anal. is a new technique of mol. marker and is widely used in plant breeding. We systematically studied the exptl. protocols and found an optimum program for rice. Using this program, exptl. time is reduced and the RAPD pattern is not changed. Also, we used the technique to analyze Thermal-Sensitive sterile rice (Annong) only one of 200 primers can amplify polymorphic patterns. We are studying the polymorphic product to confirm relation between the product and the male sterile trait.

123: 2082k **Ribosomal DNA fingerprinting analysis of Enterobacter cloacae isolated from an outbreak of nosocomial infection.** Li, Ping; Li, Guiqin; Liu, Chun; Jin, Yan; Li, Yintai; Yang, Ruifu; Guo, Zhaobiao; Li, Chonghui (Shandong Provincial Hospital, Jinan, Peop. Rep. China 250021). *Zhonghua Yufang Yixue Zazhi* 1994, 28(5), 278-80 (Ch). 16S and 23s ribosomal DNA (rDNA) genes were amplified form E. coli, labeled with [α-^{32}P] dATP by nick translation, and applied as conserved gene probes to detecting broad-spectrum rDNA. rDNA fingerprinting anal. of Enterobacter cloacae (E. cloacae) isolated form an outbreak of nosocomial infection and other

(PCR) protocol suitable for a wide range of plant species, with particular applicability to species with high polysaccharide or secondary metabolite contents.

125: 27083r **Direct PCR screening of Pichia pastoris clones.** Linder, Stefan; Schliwa, Manfred; Kube-Granderath, Eckhard (Inst. Cell Biology, Ludwig-Maximilians-Universitaet, Munich, Germany). *BioTechniques* **1996**, 20(6), 980-982 (Eng). A protocol for direct PCR screening of yeast Pichia pastoris clones is presented. One of the advantages of the protocol is that it does not require extn. and purifn. of genomic DNA, which leads to an overall and actual hands on time redn.

125: 27084s **Bi-directional dideoxy fingerprinting (bi-ddF): rapid and efficient screening for mutations in the Big Blue transgenic mouse mutation detection system.** Hasvik, Jan; Nishino, Hiroshi; Liu, Qiang; Sommer, Steve S. (Mayo Clinic/Foundation, Rochester, MN USA). *BioTechniques* **1996**, 20(6), 988, 990, 992-994 (Eng). Bi-directional dideoxy fingerprinting was applied to screen for mutations in the lacI gene, which is a target of mutagenesis in the recently developed transgenic mouse mutation detection system (Big Blue).

125: 27085t **Optimization of DNase I removal of contaminating DNA from RNA for use in quantitative RNA-PCR.** Huang, Zeqi; Fasco, Michael J.; Kaminsky, Laurence S. (Sch. Public Health, State Univ. New York, Albany, NY USA). *BioTechniques* **1996**, 20(6), 1012, 1014, 1016, 1018-1020 (Eng). In competitive RNA-PCR studies, contaminating DNA can produce incorrect results because of its potential to act as a second competitor. Preliminary studies using published methods for DNase I digestion of DNA as a contaminant of RNA, followed by thermal inactivation of the enzyme at 95° for 5 min before reverse transcription and PCR, suggested that the mRNA was also affected by these treatments. This investigation was undertaken to optimize DNase I treatment of RNA with respect to DNA removal and mRNA preservation. Competitive RNA-PCR of DT-diaphorase transcript was used to quantitate the effects of the various treatments. Other transcripts with varying initial concns. were visually compared to ensure that the effects obsd. were not unique to specific mRNAs. With 1 U of DNase I/μg RNA, thermal denaturation of the enzyme at 75° for 5 min preserved nearly all of the mRNA. Thermal denaturation at 95° for 5 min inactivated approx. 80% of the mRNA, whereas heating at 55° for 10 min did not completely denature the DNase I. For RNA-PCR of every transcript investigated, incubation of 1 μg RNA with 1 U of DNase for 30 min at 37° followed by heat-denaturation of the enzyme for 5 min at 75° was sufficient to destroy all the contaminating DNA, while completely preserving the resp. mRNAs. This treatment is highly recommended as a routine step in RNA-PCR and particularly with competitive RNA-PCR with human breast tissue samples (and presumably other human tissues), which are often contaminated with small amts. of genomic DNA.

125: 27086u **Method for 96-well M13 DNA template preparations for large-scale sequencing.** Andersson, B.; Lu, J.; Edwards, K. E.; Muzny, D. M.; Gibbs, R. A. (Baylor College Medicine, Houston, TX USA). *BioTechniques* **1996**, 20(6), 1022-1027 (Eng). Efficient prepn. of DNA templates is an important step in large-scale DNA sequencing. To ensure high-quality sequence data, M13 phage DNA templates were prepd. by using a glass fiber-filtration method. An adaptation of this protocol was applied to a 96-well format using com. available filter plates. Two variations are described: one using polyethylene glycol pptn. and a second where the phage particles are disrupted before filtration, thus eliminating the need for pptn. Using either of these protocols, 96 templates can be prepd. in <2 h. Sufficient DNA for 1-2 dye primer sequencing reactions is routinely obtained from 1 mL of culture, and the resulting sequence data are of high quality.

125: 27087v **Differential display protocol with selected primers that preferentially isolate mRNAs of moderate- to low-abundance in a microscopic system.** Ikonomov, Ognian C.; Jacob, Michele H. (Worcester Foundation, Biomedical Res., Shrewsbury, MA USA). *BioTechniques* **1996**, 20(6), 1030-1032, 1034, 1036-1042 (Eng). A modified reverse transcription polymerase chain reaction (RT-PCR)-based differential display procedure with selected primers (SPR) was developed to increase the bias toward isolating moderate- to low-abundance transcripts that are differentially expressed during synapse formation in a microscopic neuronal system, the embryonic chicken ciliary ganglion. Major modifications, in comparison with available arbitrarily primed RT-PCR protocols, include the use of (i) exptl. selected primer pairs (50% GC-rich 15-21-mers) that avoid the amplification of highly abundant ribosomal and mitochondrial transcripts; (ii) a higher PCR annealing temp. (50°C instead of 40°C); (iii) selection of sequencing gel bands that are dependent on the two primers for amplification; (i.v.) tests for reproducibility by SPR amplification of independent sets of RNA extns. and Southern blot anal. of the products with an isolated radiolabeled clone; and (v) quant. RT-PCR, instead of Northern blot anal., to confirm the differential expression of individual cDNAs. Thirty-six cDNAs were isolated and sequenced using SPR. None showed significant homol. to highly abundant transcripts. In contrast, when no criterion for primer or band selection was applied, 22% of 55 cDNAs were identical to ribosomal and mitochondrial transcripts. Reproducible amplification of 9 out of 10 SPR-isolated cDNAs was established by Southern blot anal. Differential expression was then confirmed for 4 selected sequences by quant. RT-PCR. Thus, SPR is a reproducible and efficient procedure for identifying differentially regulated transcripts of moderate- to low-abundance in microscopic biol. systems.

125: 27088w **DNA sequencing by capillary electrophoresis using short oligonucleotide primer libraries.** Ruiz-Martinez, M. C.; Carrilho, E.; Berka, J.; Kieleczawa, J.; Miller, A. W.; Foret, F.; Carson, S.; Karger, B. L. (Northeastern Univ., Boston, MA USA). *BioTechniques* **1996**, 20(6), 1058-1062, 1064, 1066-1069 (Eng). Two strategies for DNA sequencing by primer walking using short oligonucleotide primer libraries have been successfully employed along with capillary electrophoresis using replaceable polymer solns. of linear polyacrylamide and fluorescence detection. A 3.6-kb stretch of the single-stranded M13mp18 template was sequenced with T7 PRISM™ dye-terminator/Sequenase chem. An inhouse base-calling program offered read lengths of roughly 450 bases with an av. of 97.8% accuracy.

125: 27089x **Phage display shot-gun cloning of ligand-binding domains of prokaryotic receptors approaches 100% correct clones.** Jacobsson, Karin; Frykberg, Lars (Swedish Univ. Agricultural Sci., Uppsala, Swed.). *BioTechniques* **1996**, 20(6), 1070-1074, 1076, 1078-1081 (Eng). We recently presented an application of the phage display technique enabling cloning of DNA encoding ligand-binding domain(s) of prokaryotic receptors directly from chromosomal DNA. Here, we show that the use of a gene VIII-based, instead of a gene III-based, phagemid vector system results in a much more efficient selection for phage displaying a binding capacity. A phagemid library was made by insertion of randomly fragmented chromosomal DNA from Staphylococcus aureus strain 8325-4 into gene VIII in the constructed phagemid vector pG8H6. The library, which in theory should express parts of all proteins encoded by the bacterial genome, was affinity panned against the ligands IgG, fibronectin, and fibrinogen, resp. After a second panning against the same ligand, a significant increase in the no. of eluted phagemid particles was obsd., and 75%-100% of randomly picked clones contained inserts derived from genes encoding proteins with a binding affinity for the resp. ligand. The results show that this technique can be used for cloning prokaryotic receptor genes without any prior knowledge of the receptor, thus eliminating the need for probes in the identification of receptor genes.

125: 27090r **Humanized prion protein knock-in by Cre-induced site-specific recombination in the mouse.** Kitamoto, Tetsuyuki; Nakamura, Kenji; Nakao, Kazuki; Shibuya, Satoshi; Shin, Ryong-Woon; Gondo, Yoichi; Katsuki, Motoya; Tateishi, Jun (Dep. Neurological Sci., Tohoku Univ. Sch. Med., Sendai, Japan). *Biochem. Biophys. Res. Commun.* **1996**, 222(3), 742-747 (Eng). To establish humanized mice with a knock-in (gene replacement) technique, we constructed a targeting vector which consists of the human prion protein and the loxP sequences. The introduced human prion protein with the loxP system in the embryonic stem cells was transmitted through the mouse germ line. Transient expression of Cre recombinase in the fertilized eggs resulted in the prion protein humanized mice. The Cre-loxP-mediated gene replacement is a simple and efficient method which is generally applicable to make humanized animal models.

125: 27091s **A comparison of different chemiluminescent substrates for the detection of endothelial adhesion molecule transcripts.** Collie-Duguid, Elaina S. R.; Wahle, Klaus W. J. (Dept. Biochemistry, Rowett Res. Inst., Bucksburn, Aberdeen, UK AB2 9SB). *Biochem. Soc. Trans.* 1996, 24(2), 256S (Eng). Two chemiluminescent substrates, CSPD and CDP-Star, were compared for their efficiency in detecting transcripts for intercellular adhesion mol.-1 (ICAM-1), endothelial adhesion mol.-1 (E-Selectin), vascular cell adhesion mol.-1 (VCAM-1),and β-actin (control mRNA) on Northern blots by the method of P. Trayhurn et al. (1994, 1995). CDP-Star provided a higher level of sensitivity than CSPD when used to detect ICAM-1 transcripts in IL-1β-activated HUVEC cells. However, when the blot was stripped and reprobed for E-Selectin and VCAM-1 mRNAs, the prolonged exposure times required for these weaker signals resulted in a high ratio of non-specific background to signal when CDP-Star was used. When CSPD was used, each of the adhesion mol. transcripts and the β-actin transcript could be detected on the same Northern blot following stripping and reprobing.

125: 27092t **A quantitative method of determining initial amounts of DNA by polymerase chain reaction cycle titration using digital imaging and a novel DNA stain.** Becker, Andreas; Reith, Annette; Napiwotzki, Joerg; Kadenbach, Bernhard (Fachbereich Chemie, Philipps-Universitaet, D-35032 Marburg, Germany). *Anal. Biochem.* **1996**, 237(2), 204-207 (Eng). A new nonradioactive method is described for quant. detn. of small amts. of DNA by PCR, examplified with mitochondrial DNA. The method represents a combination of serial diln. PCR and kinetic PCR and avoids the use of radioactivity by applying the fluorescent dye SYBR Green I, allowing visualization of PCR amplified bands on agarose gels in a broad exponential range of PCR cycles. After recording agarose gel images with a video camera in a computer, the band intensities are processed with the NIH image program and analyzed by a new graphical method. This non radioactive method allows calcn. of small original amts. of specific DNA in samples at high accuracy.

125: 27093u **An accurate method for comparing transcript levels of two alleles or highly homologous genes: application to fibrillin transcripts in Marfan patients' fibroblasts.** Karttunen, Leena; Lonqvist, Lasse; Godfrey, Maurice; Peltonen, Leena; Syvanen, Ann-Christine (Dep. Human Molecular Genetics, National Public Health Institute, FIN-00300 Helsinki, Finland). *Genome Res.* **1996**, 6(5), 392-403 (Eng). We introduce here a novel and generally applicable, solid-phase minisequencing-based approach for rapid estn. of relative levels of transcripts with high sequence homol. This study was undertaken to screen for the consequences of different fibrillin-1 mutations on the transcripts levels in patients with the Marfan syndrome (MFS). This dominantly inherited, connective tissue disorder is characterized by

ANALYTICAL BIOCHEMISTRY 231, 359–365 (1995)

Analysis of Double-Stranded DNA by Capillary Electrophoresis with Laser-Induced Fluorescence Detection Using the Monomeric Dye SYBR Green I

Jarle Skeidsvoll[1] and Per Magne Ueland
Department of Clinical Biology, University of Bergen, Armauer Hansens Hus, N-5021 Bergen, Norway

Received April 10, 1995

The monomeric fluorescent dye, SYBR Green I, was investigated and compared with the dyes YO-PRO-1 and thiazole orange (TO) for their application in capillary electrophoresis (CE) with laser-induced fluorescence (LIF) detection of double-stranded DNA (dsDNA). DNA fragments were injected by hydrodynamic pressure and separated in a replaceable matrix of hydroxypropyl methylcellulose. For all 3 dyes, optimal concentrations were established and efficient separations of DNA fragments ranging in size from 75 to 12216 bp were obtained. The most promising results in terms of linear detection range were achieved with SYBR Green I. At the optimal dye concentration, fluorescence intensity versus DNA concentration was linear over more than three orders of magnitude (4 pg/μl to 30 ng/μl). Limit of detection (LOD) with SYBR Green I was approximately 80 fg of dsDNA (240 zmol of a 200-bp fragment). Similar LOD was obtained with YO-PRO-1, whereas TO resulted in lower sensitivity. Precision in both fluorescence intensity and migration time was high (relative standard deviation, RSD < 3.6%; $n = 10$) for dsDNA fragments complexed with SYBR Green I. In conclusion, SYBR Green I is a fluorescent dye well suited for efficient separation and quantitative, sensitive, and precise determination of dsDNA by CE–LIF.

Capillary electrophoresis (CE)[2] represents a significant improvement in electrophoretic analysis of nucleic acids in terms of speed, resolution, quantitation, reproducibility, and automation compared with conventional gel electrophoresis systems (1,2). Highly efficient separations of single- and double-stranded DNA ranging in size from a few nucleotides to millions of base pairs have been obtained by CE (3,4).

Due to the minute sample volumes injected in typical CE analyses (nanoliter range), the practical application of CE is highly dependent on sensitive detection systems. Detection by uv absorbance is commonly used in CE analyses of DNA, but confers limited sensitivity. Extremely high sensitivity can be obtained by laser-induced fluorescence (LIF) detection (5). This approach requires fluorescent DNA derivatives obtained by either covalent binding of fluorophores or physical absorption of fluorogenic dyes.

Characteristics of an ideal fluorescent dye for CE–LIF analysis of DNA have been summarized by Schwartz and Ulfelder (6) as (1) excitation maximum of the DNA–dye complex close to a available laser wavelength, (2) low intrinsic fluorescence of dye not complexed with DNA, (3) large fluorescence enhancement upon binding of dye to DNA, and (4) high fluorescence quantum yield of the DNA–dye complex. Additional important characteristics for quantitation of DNA in unknown samples are (5) uniform and not sequence specific binding, (6) constant fluorescence intensity and electropherographic profile over a wide range of DNA–dye ratios, and (7) large linear detection range.

A series of new fluorescent dyes with improved physical and spectroscopic properties have recently been developed (7–10). The dyes can be classified as monomeric and dimeric. The dimeric dyes have several favorable features, including high affinity for and large fluorescence enhancement upon binding dsDNA (10). However, efficient separations are only obtained over

[1] To whom correspondence should be addressed. Fax: +47-55-974605.

[2] Abbreviations used: CE, capillary electrophoresis; LIF, laser-induced fluorescence; YO-PRO-1, 1-(4-[3-methyl-2,3-dihydro-(benzo-1,3-oxazole)-2-methylidene]-quinolinium)-3-trimethylammonium propane diodide; TO, thiazole orange; LOD, limit of detection; DMSO, dimethyl sulfoxide; HPMC, hydroxypropyl methylcellulose.

0003-2697/95 $12.00

a narrow range of DNA–dye ratios, and broad and distorted peaks attributed to multiple complex formation modes are obtained if not proper measures are taken (11,12).

Among the monomeric dyes, the intercalator, ethidium bromide, has been found to improve peak shape and resolution in CE of dsDNA (13). Recently, the monomeric dyes 1-(4-[3-methyl-2,3-dihydro-(benzo-1,3-oxazole) - 2 - methylidene] - quinolinium) - 3 - trimethylammonium propane diodide (YO-PRO-1) and thiazole orange (TO; 4-[3-methyl-2,3-dihydro-(benzo-1,3-thiazole)-2-methylidene]-quinolinium iodide) were evaluated (6,14). TO intercalates dsDNA at a ratio of one dye molecule per two base pairs of DNA (8). High sensitivity detection and high resolution of dsDNA fragments have been obtained with both fluorescent dyes (6,14).

SYBR Green I is the trade name of a new ultrasensitive monomeric dye developed for the detection of dsDNA in agarose and polyacrylamide gels. SYBR Green I has several attractive properties, including excitation maximum close to the 488 nm line of the argon ion laser, extremely low intrinsic fluorescence, high fluorescence quantum yield of the DNA–dye complex, and 100-fold higher affinity for dsDNA than ethidium bromide (7).

In the present work we demonstrate for the first time the applicability of SYBR Green I for separation and quantitation of dsDNA by CE–LIF. Important features of SYBR Green I are compared with those of the cyanine dyes YO-PRO-1 and TO. The most prominent advantages of SYBR Green I are large linear detection range of dsDNA and high resolution of small dsDNA fragments.

MATERIALS AND METHODS

Chemicals

SYBR Green I (in dimethyl sulfoxide (DMSO); concentration not given) and YO-PRO-1 (1 mM in DMSO) were purchased from Molecular Probes Inc. (Eugene, OR). TO was a gift of Molecular Probes, and is at present not commercially available. TO was dissolved in methanol (Rathburn Chemicals Ltd., Walkerburn, Scotland) to a final concentration of 2 mM.

Working stock solutions of SYBR Green I (1:100 dilution of stock), YO-PRO-1 (10 μM) and TO (10 μM) in 20% DMSO (E. Merck, Darmstadt, Germany) were prepared daily, and stored in the dark at room temperature.

Phenylmethylpolysiloxane-coated fused silica capillaries (DB-17, 100 μm i.d., 0.1 μm film thickness) were purchased from J & W Scientific (Folsom, CA). Wizard PCR Preps DNA Purification System was purchased from Promega Corp. (Madison, WI). Acrodisc PVDF filters (0.45 μm pore size) were from Gelman Sciences Inc. (Ann Arbor, MI) and MF-Millipore membrane filters (0.025 μm pore size, 10 mm diameter) were from Millipore Corp. (Bedford, MA). Hydroxypropyl methylcellulose (HPMC, 4000 cP, 2% aqueous solution, 25°C) and other chemicals (molecular biology grade) were obtained from Sigma Chemical Co. (St. Louis, MO). Solutions containing HPMC were prepared as described elsewhere (15). Reagents and reaction tubes (Thin-Walled GeneAmp) for PCR were purchased from Perkin Elmer (Norwalk, CT). Water, double distilled and purified on a Milli-Q Plus Water Purification System (Millipore), was used for preparation of all aqueous solutions.

Capillary Electrophoresis Instrumentation

Capillary electrophoresis was performed on a Beckman P/ACE System 2100 equipped with P/ACE LIF detector (Beckman Instruments, Palo Alto, CA). Laser excitation was at 488 nm (argon ion laser, 3 mW, Beckman Instruments). The emitted light was collected by passage through 488 nm blocking and 520 nm bandpass filters (bandwidth 10 nm) (Beckman Instruments).

Total capillary length was 27 cm (20 cm effective length). Capillary electrophoresis was performed in the reversed polarity mode with capillary temperature set at 18°C.

Beckman System Gold software (version 7.12) was used for system control, data collection, and processing. Electropherograms for preparation of figures were transferred as DIF files to an Apple Macintosh computer and redrawn by Sigma Plot (version 4.16; Jandel Scientific GmbH, Erkrath, Germany).

DNA Molecular Size Standards

The 1 kb DNA Ladder (1.04 μg/μl) and DNA Mass Ladder (117.5 ng/μl) were from Life Technologies Inc. (Gaithersburg, MD). The 1 kb DNA Ladder contains 21 DNA fragments ranging in size from 75 to 12216 bp, whereas the DNA Mass Ladder is an equimolar composition of 100-, 200-, 400-, 800-, 1200-, and 2000-bp DNA fragments. The DNA standards were diluted to appropriate concentrations in purified water and stored at 4°C.

Polymerase Chain Reaction and Purification of the Product

A 210-bp segment originating from N-terminus of the human chromosomal *mut* gene (16) was amplified using the following protocol: A 100-μl reaction volume containing 100 pg of the MCM26 plasmid (16), 100 pmol of each primer, 200 μM dNTPs, 50 mM KCl, 10 mM Tris–HCl (pH 8.3), 1.5 mM $MgCl_2$, 0.001% (w/v) gelatin and 2 U AmpliTaq DNA Polymerase (Perkin Elmer) was subjected to 36 temperature cycles on a DNA Thermal Cycler 480 (Perkin Elmer). PCR ther-

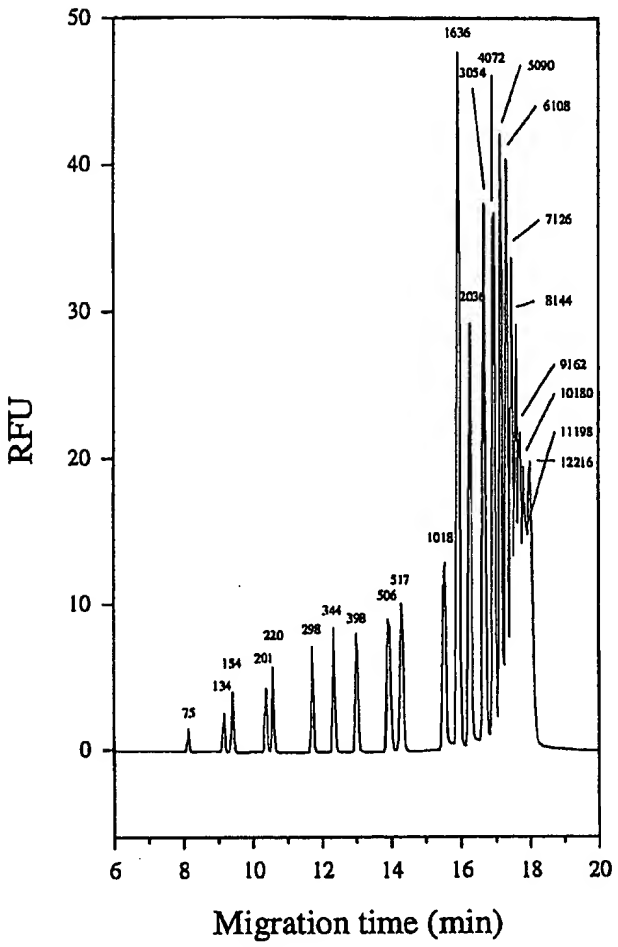

FIG. 1. Electropherogram of the 1 kb DNA Ladder complexed with SYBR Green I. The concentration of SYBR Green I in electrophoresis and separation buffers corresponds to a 1:30,000 dilution of stock solution. Total DNA concentration, 10 ng/μl (corresponding to 200 pg of DNA injected). Other experimental conditions as described under Materials and Methods. RFU, relative fluorescence units.

mocycling program: 1 min at 94°C (initial denaturation), followed by 36 temperature cycles of 1 min at 94°C (denaturation), 1 min at 45°C (primer annealing), and 1 min at 72°C (primer extension). Final primer extension was 7 minutes at 72°C.

If not otherwise stated, PCR samples were purified by Wizard PCR Preps DNA Purification System (Promega) and dialyzed on a MF-Millipore membrane filter (Millipore) for 20 min (17) prior to analysis by capillary electrophoresis. For determination of linear detection ranges, the PCR product was initially quantitated by uv spectrophotometry and then diluted in purified water to appropriate concentration.

Capillary Electrophoresis

Electrophoresis buffer was 89 mM Tris–borate, 2 mM EDTA, pH 8.3 (1× TBE). Separation buffer was electrophoresis buffer containing 0.5% (w/v) HPMC. All buffers were passed through Acrodisc PVDF filters and degassed by sonication for 10 min prior to CE. A significant adsorption of dye to filter matrix was observed if dye was added before filtration. Fluorescent dye was added to both electrophoresis and separation buffers.

The capillary was filled with separation buffer by high-pressure injection at 137 kPa (20 psi) for 30 s, followed by a short immersion in purified water (to prevent carryover of buffer salts and HPMC). Samples were injected by low pressure at 3.44 kPa (0.5 psi) for 10 s and separation performed at an electric field strength of 180 V/cm. After each electroseparation, the capillary was flushed with 1× TBE for 60 s by high pressure. For direct analysis of PCR reaction mixtures, purified water was injected (low pressure, 10 s) prior to the PCR sample. This procedure has been advocated to prevent matrix effect (18).

In order to obtain quantitative data from the on-line detection system, fluorescence intensity from analytes having different mobilities were normalized by using the product of fluorescence intensity and mobility for each of the analytes. All data presented here were normalized by the System Gold software.

RESULTS AND DISCUSSION

Capillary Electrophoresis System

The aim of this study was to investigate the properties of monomeric SYBR Green I as a fluorescent dye for quantitative analysis of dsDNA by CE–LIF and compare SYBR Green I with the two monomeric dyes, YO-PRO-1 and TO.

Hydrodynamic injection of sample was used since this allowed quantitative introduction of dsDNA fragments of different sizes dissolved in matrices of variable ionic strength (18,19). Using the Poiseuille equation, we estimated that a 10-s low-pressure injection introduced approximately 20 nl of sample into the capillary. Hydrodynamic injection is only possible with replaceable separation matrices. Preliminary experiments demonstrated that a HPMC concentration of 0.5% in the separation buffer and an electric field

TABLE 1

Excitation and Emission Maxima of SYBR Green I, YO-PRO-1, and TO Complexed with DNA

Fluorescent dye	Excitation maximum (nm)	Emission maximum (nm)
SYBR Green I	494	521
YO-PRO-1	491	509
TO	509	525

strength of 180 V/cm gave acceptable separation of DNA fragments ranging in size from 75 to 12216 bp (Fig. 1), and that resolution in the lower and higher size range could be further improved by increasing (to 1%) or decreasing (to 0.2%) the concentration of HPMC, respectively.

The DNA–dye complexes have excitation maxima (494 nm, SYBR Green I; 491 nm, YO-PRO-1 (9); 509 nm, TO (8)) close to the 488-nm line of the argon ion laser used in these experiments. The emission maxima of these dyes are in the range of 509–525 nm (Table 1). The emitted light was directed through a bandpass filter (520 ± 5 nm) which collected light with intensity 50–100% of the emission maxima.

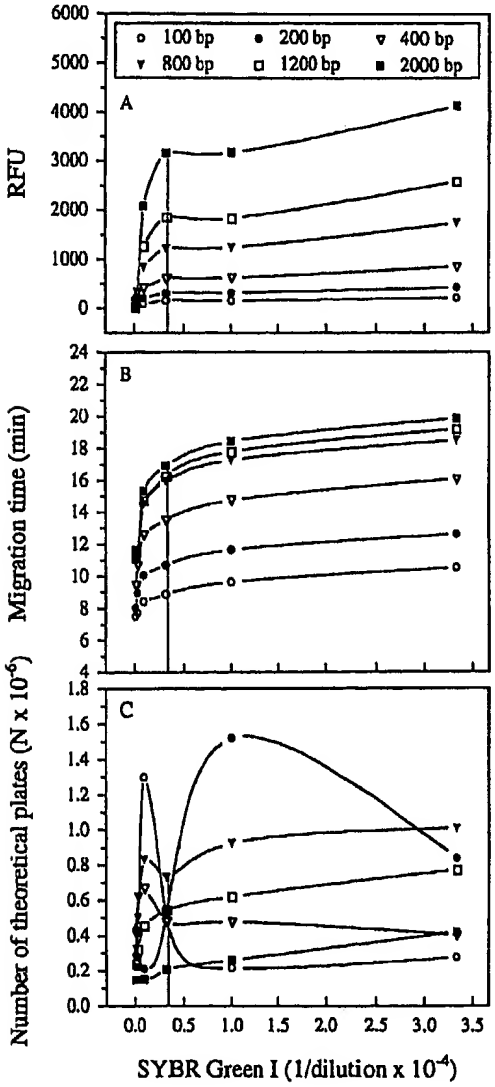

FIG. 2. Effect of SYBR Green I concentration on fluorescence intensity, migration time, and plate numbers for dsDNA fragments. The DNA Mass Ladder at a total DNA concentration of 10 ng/μl was subjected to CE–LIF in the presence of increasing concentrations of SYBR Green I in electrophoresis and separation buffers. Other experimental conditions were as described in the legend to Fig. 1. SYBR Green I concentration corresponding to a 1:30,000 dilution of stock solution is indicated by a vertical dotted line. The fluorescence intensity was normalized for the analytes. RFU, relative fluorescence units.

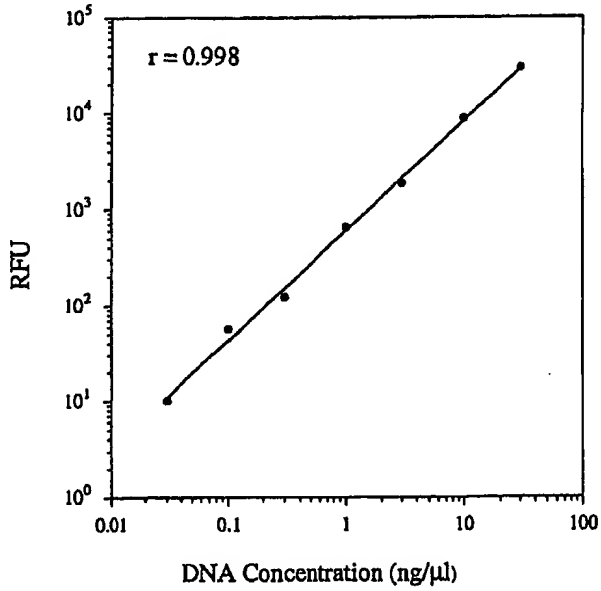

FIG. 3. Linear detection range. A 210-bp PCR amplified segment of the *mut* gene was subjected to CE in the presence of SYBR Green I concentration corresponding to a 1:30,000 dilution of stock solution. The concentration of DNA varied between 0.025 and 25 ng/μl, as indicated on the abscissa. Other experimental conditions were as described in the legend to Fig. 1. RFU, relative fluorescence units.

Optimization of Dye Concentration

Absorption of monointercalators induces structural and electrostatic changes in dsDNA (20), resulting in altered migration dynamics when the complexes are subjected to electrophoresis. Separation characteristics depend on the stoichiometric relations between DNA base pairs and intercalating dye molecules (13). Consequently, an optimal DNA–dye ratio in terms of peak resolution, R_S, and plate number, N will exist.

We investigated the effect of increasing fluorescent dye concentrations on fluorescence intensity, migration time, and separation characteristics in CE–LIF of DNA molecular weight standards.

The fluorescence intensity and migration time for DNA fragments ranging from 100 to 2000 bp increased with SYBR Green I concentration up to a dilution of 1:100,000–1:30,000. Higher dye concentration caused only small further increase in these parameters (Figs. 2A and 2B). Shift in migration times was positively correlated to fragment size (Fig. 2B).

TABLE 2

Limit of Detection and Linear Detection Range of DNA Analysis with SYBR Green I, YO-PRO-1, and TO

Fluorescent dye	Limit of detection (fg)[a]	Linear detection range (ng/μl)
SYBR Green I	80	0.004–30
YO-PRO-1	80	0.004–12
TO	850	0.042–12

[a] Determined for a 200-bp DNA fragment of the DNA Mass Ladder.

The plate numbers increased for all fragments up to a SYBR Green I dilution of 1:100,000. At dilutions between 1:100,000 and 1:3000, the plate numbers for the different DNA fragments showed a complex relation to dye concentration, as depicted in Fig. 2C. We routinely used SYBR Green I at a dilution of 1:30,000 which, in addition to high fluorescence intensity, resulted in the highest resolution (R_S) of DNA fragments up to 1000 bp (R_S = 1.5 for the 506/517 bp fragments). Under these optimized conditions, we obtained baseline separation of the 134/154, 201/220, and 506/517 bp doublets (Fig. 1).

The fluorescence intensities and migration times for DNA fragments ranging from 100 to 2000 bp increased with YO-PRO-1 and TO concentrations up to 300 nM (for both dyes) and then leveled off (data not shown). The increment in migration times, attributed to combined mass and charge effects due to complex formation, was most pronounced for the higher molecular weight fragments.

The dye concentration 300 nM was also found to be optimal with respect to plate numbers for YO-PRO-1 and TO (data not shown). Increasing the dye concentrations beyond the optimal level caused the loss of system efficiency. At TO concentrations higher than 1 μM, there was a marked deterioration of peak shape and a significant reduction in plate numbers for DNA fragments smaller 400 bp (data not shown). This observation is essentially in agreement with published data (6).

At low concentrations of SYBR Green I (diluted >1:100,000) and YO-PRO-1 (<100 nM), we observed a selective loss of fluorescence from DNA fragments larger than 400 bp and a significant reduction in their migration times (data not shown). This phenomenon has previously been described for YO-PRO-1, and is attributed to depletion of dye by complex formation with the faster migrating fragments (14). Almost quantitative extraction of dye from the separation buffer at low concentrations of SYBR Green I and YO-PRO-1 probably reflects their high affinity for dsDNA. This phenomenon was not observed with TO which have lower affinity for dsDNA.

Linear Detection Range

Optimal concentrations of SYBR Green I (dilution 1:30,000), YO-PRO-1 (300 nM) and TO (300 nM) were established at a total DNA concentration of 10 ng/μl. We further investigated the fluorescence intensity over a large concentration range of dsDNA (0.1 ng to 100 ng/μl) at optimal concentrations of the fluorescent dyes. The DNA Mass Ladder and a 210-bp PCR amplified

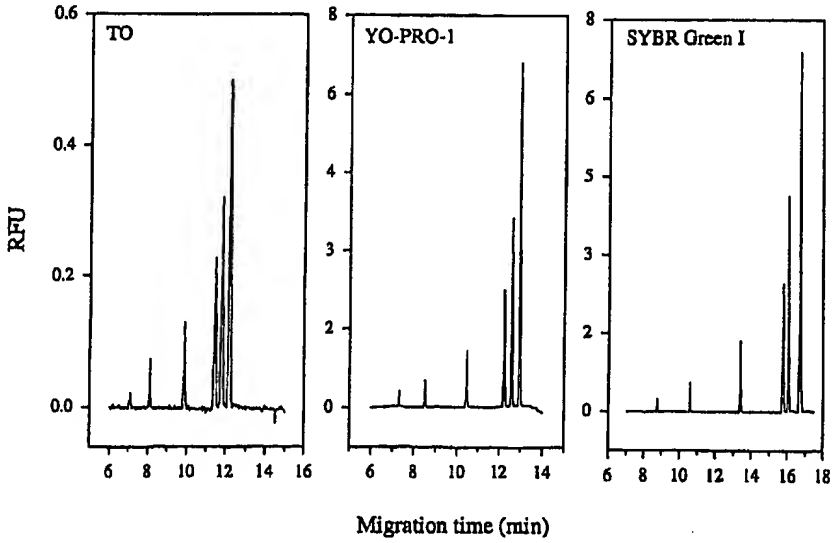

FIG. 4. Electropherografic profiles obtained with TO, YO-PRO-1, and SYBR Green I. The DNA Mass Ladder at a total concentration of 1 ng/μl was subjected to CE in the presence of optimal concentrations of TO (300 nM), YO-PRO-1 (300 nM), or SYBR Green I (a 1:30,000 dilution of stock solution). Other experimental conditions were as described in the legend to Fig. 1. RFU, relative fluorescence units.

TABLE 3

Precision of DNA Analysis with SYBR Green I, YO-PRO-1, and TO

Fluorescent dye	DNA fragment size (bp)	RSD, migration time (%)[a]	RSD, fluorescence intensity (%)[a]
SYBR Green I	200	0.46	3.3
	800	0.48	3.2
	2000	0.49	3.6
YO-PRO-1	200	0.95	5.6
	800	1.14	8.4
	2000	1.15	8.6
TO	200	0.46	9.9
	800	0.63	11
	2000	0.62	12

[a] Data were obtained from 10 repetitive injections of a single sample (n = 10).

DNA segment of the *mut* gene were used for these experiments.

The fluorescence intensity of DNA fragments complexed with SYBR Green I increased linearly as a function of DNA concentration over three orders of magnitude. Figure 3 illustrates the large linear range (25 pg/μl to 25 ng/μl) for detection of the 210-bp PCR product. Notably, the linear ranges obtained with YO-PRO-1 and TO were smaller (Table 2). The migration times and separation characteristics were essentially constant within these DNA concentration ranges (data not shown).

The linearity in fluorescence intensity versus DNA concentration observed for the monomeric dyes investigated here is explained by a constant amount of dye per fragment over a wide range of DNA–dye ratios. This contrasts to the variable intensity obtained when using constant concentration of dimeric dyes at different DNA–dye ratios (11).

In conventional gel electrophoresis, the fluorescence intensity from dsDNA fragments complexed with intercalating dyes of weak base specificity has been found to be linearly related to the fragment size. We made analogous observations with SYBR Green I and YO-PRO-1. For these dyes, the fluorescence intensity per base pair was independent of DNA fragment size, indicating uniform binding to dsDNA. In contrast, using TO as intercalator, the fluorescence intensity per base pair was highest for the smallest fragments and decreased with fragment size. This phenomenon was observed with both DNA molecular size standards analyzed and over a wide range of DNA concentrations (0.1 to 100 ng/μl) (data not shown).

The relation between DNA fragment size and fluorescence intensity can have practical implications for the construction of quantitative methods for dsDNA based on CE–LIF. The fluorescence intensity per base pair is not dependent on the size of dsDNA fragments complexed with SYBR Green I, thus providing greater freedom in selection of internal standard (in terms of molecular weight).

Performance of DNA Analysis

Limits of detection (signal to noise ratio of 3:1, 3σ) of a 200-bp DNA fragment were approximately 80 fg

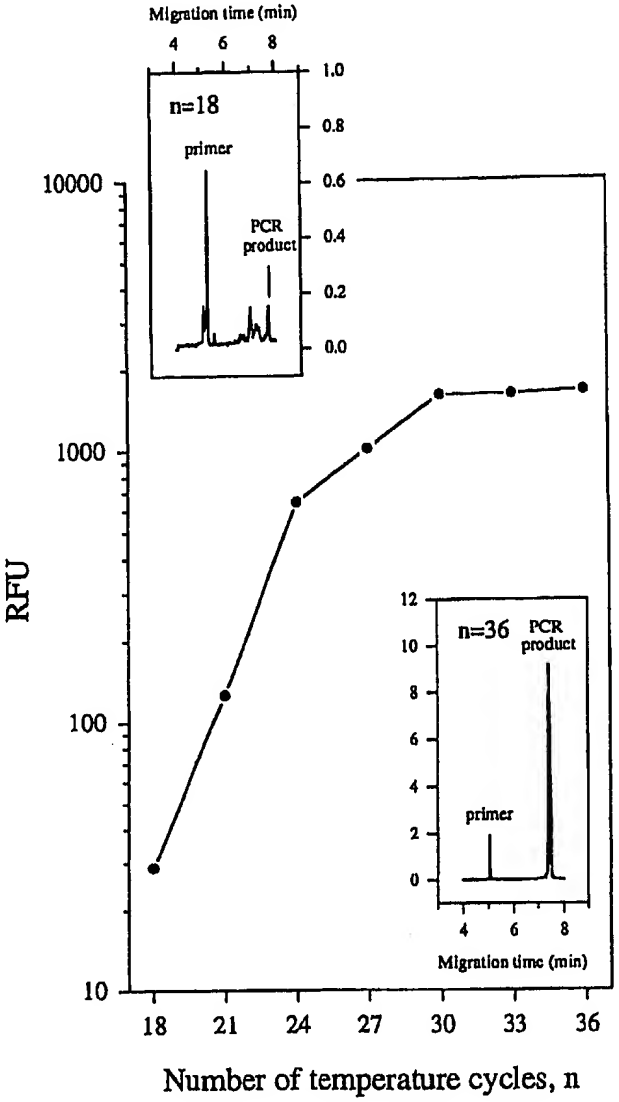

FIG. 5. Monitoring PCR amplification. A 210-bp segment of the *mut* gene was amplified by PCR as described under Materials and Methods. Samples from parallel PCR reactions were injected by hydrodynamic pressure (10 s at 3.44 kPa) without prior purification. CE was performed with SYBR Green I (a 1:30,000 dilution of stock solution) in the electrophoresis and separation buffers. The main panel illustrates the progress curve for the PCR reaction, whereas the insets illustrate electropherograms of reaction mixtures after 18 and 36 temperature cycles, respectively. RFU, relative fluorescence units.

with SYBR Green I and YO-PRO-1 and approximately 850 fg with TO (Table 2). The higher sensitivity obtained with SYBR Green I and YO-PRO-1 is also demonstrated by comparing electropherograms of the DNA Mass Ladder (total DNA concentration 1 ng/μl) (Fig. 4).

Construction of the LIF detection system is an obvious determinant of sensitivity. We used a commercial detector which does not fully exploit the potential of LIF detection (21). Previous studies have shown that the cyanine fluorophores TO and the YO-PRO-1 analog, YO, give 10-fold higher sensitivity than ethidium and its derivatives, propidium-2 and propidium-3 (11). Thus, SYBR Green I seems to compare favorably with established intercalating dyes previously used in CE–LIF (11,12).

Precision of fluorescence intensity and migration time was determined by repetitive (n = 10) hydrodynamic injections of the DNA Mass Ladder. The relative standard deviation was between 3.3 and 12% for fluorescence intensity and 0.46 and 1.2% for migration time (Table 3).

Monitoring PCR Amplification of the mut Gene

We monitored PCR amplification of a 210-bp segment of the human *mut* gene through 36 temperature cycles by analyzing the reaction products by CE–LIF. Samples were analyzed without prior purification and detected by complex formation with SYBR Green I. The product, detected after 18 cycles, was efficiently separated from unreacted primers and interfering material (Fig. 5). The results demonstrated rapid, quantitative, and precise determination of PCR products detected by the use of SYBR Green I.

CONCLUSION

Excitation maximum of the dsDNA–SYBR Green I complex is close to the 488-nm line of the argon ion laser. SYBR Green I has low intrinsic fluorescence and large fluorescence enhancement upon binding to dsDNA. At optimal concentrations (dilution 1:30,000) of SYBR Green I, efficient separation and sensitive detection of dsDNA fragments are obtained by CE–LIF over a wide range of DNA–dye ratios. YO-PRO-1 and TO also serve as useful dyes for dsDNA analysis by CE–LIF. Compared with these dyes, the most prominent advantages of SYBR Green I are the high resolution of DNA fragments 100–1000 bp in size and a large linear detection range. The latter feature is a prerequisite for quantitative measurement of DNA samples.

ACKNOWLEDGMENTS

This work was supported by grants from the Norwegian Cancer Association. The technical assistance of Gry Kvalheim is highly appreciated. We also thank Dr. Singer at Molecular Probes for useful discussions.

REFERENCES

1. Kuhr, W. G., and Monnig, C. A. (1992) *Anal. Chem.* **64**, 389R–407R.
2. Monnig, C. A., and Kennedy, R. T. (1994) *Anal. Chem.* **66**, 280R–314R.
3. Sudor, J., and Novotny, M. V. (1994) *Anal. Chem.* **66**, 2446–2450.
4. Heiger, D. N., Cohen, A. S., and Karger, B. L. (1990) *J. Chromatogr.* **516**, 33–48.
5. Chen, D. Y., Adelheim, K., Cheng, X. L., and Dovichi, N. J. (1994) *Analyst* **119**, 349–352.
6. Schwartz, H. E., and Ulfelder, K. J. (1992) *Anal. Chem.* **64**, 1737–1740.
7. Singer, V., Jin, X., Ryan, D., and Yue, S. (1994) *BioMed. Prod.* **April**, 68–72.
8. Lee, L. G., Chen, C., and Chiu, L. A. (1986) *Cytometry* **7**, 508–517.
9. Haugland, R. P. (1992–1994) *In* Handbook of Fluorescent Probes and Research Chemicals (Larison, K. D., Eds.), 5th ed., pp. 221–234, Molecular Probes, Inc., Eugene, OR.
10. Rye, H. S., Yue, S., Wemmer, D. E., Quesada, M. A., Haugland, R. P., Mathies, R. A., and Glazer, A. N. (1992) *Nucleic Acids Res.* **20**, 2803–2812.
11. Zhu, H., Clark, S. M., Benson, S. C., Rye, H. S., Glazer, A. N., and Mathies, R. A. (1994) *Anal. Chem.* **66**, 1941–1948.
12. Kim, Y., and Morris, M. D. (1994) *Anal. Chem.* **66**, 1168–1174.
13. Guttman, A., and Cooke, N. (1991) *Anal. Chem.* **63**, 2038–2042.
14. McCord, B. R., McClure, D. L., and Jung, J. M. (1993) *J. Chromatogr.* **652**, 75–82.
15. Baba, Y., Ishimaru, N., Samata, K., and Tsuhako, M. (1993) *J. Chromatogr.* **653**, 329–335.
16. Jansen, R., Kalousek, F., Fenton, W. A., Rosenberg, L. E., and Ledley, F. D. (1989) *Genomics* **4**, 198–205.
17. Williams, P. E. (1992) *Methods* **4**, 227–232.
18. Butler, J. M., McCord, B. R., Jung, J. M., Wilson, M. R., Budowle, B., and Allen, R. O. (1994) *J. Chromatogr. B* **658**, 271–280.
19. Huang, X., Gordon, M. J., and Zare, R. N. (88) *Anal. Chem.* **60**, 375–377.
20. Watson, J. D., Hopkins, N. H., Roberts, J. W., Steitz, J. A., and Weiner, A. M. (1987) Molecular Biology of the Gene, Benjamin–Cummings, Redwood City, CA.
21. Toulas, C., and Hernandez, L. (1992) *LC-GC* **10**, 471–476.